

**SIMULATION, INTEGRATION, AND ECONOMIC
ANALYSIS OF GAS-TO-LIQUID PROCESSES**

A Thesis

by

BUPING BAO

Submitted to the Office of Graduate Studies of
Texas A&M University
in partial fulfillment of the requirements for the degree of

MASTER OF SCIENCE

December 2008

Major Subject: Chemical Engineering

**SIMULATION, INTEGRATION, AND ECONOMIC
ANALYSIS OF GAS-TO-LIQUID PROCESSES**

A Thesis

by

BUPING BAO

Submitted to the Office of Graduate Studies of
Texas A&M University
in partial fulfillment of the requirements for the degree of

MASTER OF SCIENCE

Approved by:

Chair of Committee,	Mahmoud M. El-Halwagi
Committee Members,	Nimir Elbashir
	M. Sam Mannan
	Guy Curry
Head of Department,	Michael Pishko

December 2008

Major Subject: Chemical Engineering

ABSTRACT

Simulation, Integration, and Economic Analysis of
Gas-to-Liquid Processes. (December 2008)

Buping Bao, B.S., Zhejiang University

Chair of Advisory Committee: Dr. Mahmoud M. El-Halwagi

Gas-to-liquid (GTL) process involves the chemical conversion of natural gas (or other gas sources) into synthetic crude that can be upgraded and separated into different useful hydrocarbon fractions including liquid transportation fuels. A leading GTL technology is the Fischer Tropsch process. The objective of this work is to provide a techno-economic analysis of the GTL process and to identify optimization and integration opportunities for cost saving and reduction of energy usage and environmental impact. First, a base-case flowsheet is synthesized to include the key processing steps of the plant. Then, computer-aided process simulation is carried out to determine the key mass and energy flows, performance criteria, and equipment specifications. Next, energy and mass integration studies are performed to address the following items: (a) heating and cooling utilities, (b) combined heat and power (process cogeneration), (c) management of process water, (d) optimization of tail-gas allocation, and (e) recovery of catalyst-supporting hydrocarbon solvents. Finally, an economic analysis is undertaken to determine the plant capacity needed to achieve the break-even point and to estimate the return on investment for the base-case study. After integration, 884 million \$/yr is saved from heat integration, 246 million \$/yr from heat cogeneration, and 22 million \$/yr from water management. Based on 128,000 barrels per day (BPD) of products, at least 68,000 BPD capacity is needed to keep the process profitable, with the return on investment (ROI) of 5.1%. Compared to 8 \$/1000 SCF natural gas, 5 \$/1000 SCF price can increase the ROI to 16.2%.

ACKNOWLEDGEMENTS

I would like to thank all those who gave me the possibility to complete this thesis. First, I want to express my sincere and utmost gratitude to my advisor, Dr. El-Halwagi, not only for his insightful suggestions throughout my research, but also for his patience and generous support during my graduate years. I owe a great deal to him. Without his spiritual guidance and invaluable advice, I would not have gone as deep into the research nor realized the essence of chemical process engineering. His passion for process research, enthusiastic attitude to people, and wisdom set an example for me.

I am especially obliged to my committee members for their support and advice. I appreciate Dr. Elbashir very much for offering me the chance to simulate the F-T solvent recovering and for his kindness to give me detailed explanations to my questions. I also want to thank Dr. Mannan and Dr. Curry for their careful and kind instruction in coursework and research. Their dedication and professional spirit moves me.

I would like to extend my gratitude to all the staff in the department, especially Towanna, who has never been bothered by helping me with documents and has always provided me with tremendous help. I cannot thank her enough.

I further have to thank the process integration group and colleagues: Eman, Denny, Viet, Ting, Arwa, Grace, and Jose, for their help and support. Their accompaniment made my research life delightful and cheerful.

Finally, I am deeply indebted to my parents, who support me unconditionally when I am depressed and nervous. It is their encouragement and love that leads me to insist, to strive all the way toward my goal, and to stick to my interests and dreams.

NOMENCLATURE

ASF	Anderson-Schulz-Flory Equation
ASU	Air Separation Unit
ATR	Autothermal Reactor
bbl	Barrels
BPD	Barrels Per Day
BSCFD	Standard Cubic Feet per Day
CAPEX	Capital Expenditures
CFB	Circulating Fluidized Bed
EIA	Energy Information Administration
FCI	Fixed Capital Investment
F-T	Fischer Tropsch
gal	Gallon
GTL	Gas to Liquid
HEN	Heat Exchange Network
HP	High Pressure
hr	Hour
HTFT	High Temperature Fischer Tropsch
IGCC	Integrated Gasification Combined Cycle
kg	Kilogram
kWh	Kilowatt Hour
lb	Pound
LNG	Liquefied Natural Gas
LP	Low Pressure
LPG	Liquefied Petroleum Gas
LTFT	Low Temperature Fischer Tropsch
MEN	Mass Exchange Network
MILP	Mixed Integer Linear Program

MMBtu	Million British Thermal Unit
MMTPA	Million Tones Per Year
POX	Partial Oxidation
ROI	Return On Investment
SAS	Sasol Advanced Synthol
SMDS	Shell Middle Distillate Synthesis
SMR	Steam Methane Reforming
SPD	Slurry-Phase Distillate Process
TAC	Total Annualized Cost
TCI	Total Capital Investment
TEHL	Table of Exchangeable Heat Loads
TID	Temperature Interval Diagram
ton	Tonne
WGS	Water Gas Shift
yr	Year
\$	Dollar

TABLE OF CONTENTS

	Page
ABSTRACT	iii
ACKNOWLEDGEMENTS	iv
NOMENCLATURE	v
TABLE OF CONTENTS	vii
LIST OF FIGURES	ix
LIST OF TABLES	xi
1 INTRODUCTION	1
1.1 Interest and Background	1
1.2 Basic Process Steps	3
1.3 Historical Development	12
1.4 Literature Review	16
1.5 Relevant Features	18
2 PROBLEM STATEMENT	27
3 METHODOLOGY AND APPROACH	29
3.1 Overview of the Design Approach	29
3.2 Methodology on Formulation for MEN & HEN Retrofitting	32
4 CASE STUDY	51
4.1 GTL Process Description	51
4.2 Design Basis and Specifications	52
5 RESULTS AND ANALYSIS	56
5.1 Process Synthesis and Alternative Operating Condition Analysis	56
5.2 Process Mass and Heat Balance	58
5.3 Heat Integration and Targeting	59
5.4 Heat Engine and Cogeneration Targeting	63

	Page
5.5 Mass Integration.....	68
5.6 Total Cost for GTL Plant	74
6 CONCLUSIONS AND RECOMMENDATIONS.....	81
REFERENCES.....	83
VITA	91

LIST OF FIGURES

		Page
Figure 1.1	Environmental advantages of GTL processes compared to normal diesel.....	3
Figure 1.2	GTL process in chemistry	4
Figure 1.3	Energy consumption of each unit for GTL process	5
Figure 1.4	ASF distribution of GTL products with log scheme	7
Figure 1.5	F-T reactors	10
Figure 1.6	Sasolburg GTL process	14
Figure 1.7	CO ₂ from each unit.....	17
Figure 2.1	Schematic representation of the problem statement.....	28
Figure 3.1	Overview of the GTL process analysis	29
Figure 3.2	Hierarchical design approach	30
Figure 3.3	Process synthesis problems	32
Figure 3.4	Process analysis problems.....	33
Figure 3.5	Process from species perspective when integrated.....	36
Figure 3.6	Identifying pinch point for maximum recycling	38
Figure 3.7	Cascade diagram for mass integration	39
Figure 3.8	Heat exchange network (HEN) synthesis.....	40
Figure 3.9	Thermal pinch diagram	42
Figure 3.10	Temperature-interval diagram.....	43
Figure 3.11	Heat balance around a temperature interval	44

	Page
Figure 3.12 Cascade diagram for HENs	46
Figure 3.13 Placing of the heat engine for the HEN.....	47
Figure 3.14 Overview of the strategies for the application	48
Figure 3.15 Extractable power cogeneration targeting pinch diagram.....	50
Figure 4.1 Schematic representation of the base-case GTL flowsheet.....	51
Figure 4.2 Products distribution following ASF.....	54
Figure 4.3 Products boiling point curve	54
Figure 5.1 GTL process flowsheet.....	56
Figure 5.2 Description of the hot and cold streams	59
Figure 5.3 Temperature interval diagram for the GTL process.....	61
Figure 5.4 Cascade diagram for the GTL process	64
Figure 5.5 Grand composite curve for the GTL process	65
Figure 5.6 Integrating of the heat engine with HEN	66
Figure 5.7 Unshifted extractable power versus flowrate plot.....	67
Figure 5.8 Representation of the cogeneration flowsheet	67
Figure 5.9 Assignment of split fractions and assignment to sinks for GTL process.....	69
Figure 5.10 Solvent recoverability from the flash as a function of temperature and pressure.....	71
Figure 5.11 C ₁₀₊ increase with temperature and pressure change in the flash.....	71
Figure 5.12 Flowsheet for solvent recovering	72
Figure 5.13 Break-even point calculation.....	80

LIST OF TABLES

		Page
Table 1.1	Comparison between GTL and LNG	2
Table 1.2	Example of a pilot F-T product distribution.....	8
Table 1.3	Features for each F-T reactor	11
Table 1.4	List of GTL commercial development	14
Table 1.5	Comparison of different types of F-T reactors	18
Table 1.6	The features for each catalyst.....	22
Table 1.7	Distillation range for LTFT synthesis crude (or syncrude) fractions.....	24
Table 4.1	The feed gas conditions.....	52
Table 4.2	Composition of the products from the F-T reactor	53
Table 4.3	Conditions and costs of the heating and cooling utilities.....	55
Table 5.1	Syncrude fractions.....	57
Table 5.2	Compositions (mass%) of the streams leaving the distillation columns	58
Table 5.3	Mass balance for GTL process.....	58
Table 5.4	Heat duty for each unit in the GTL process	59
Table 5.5	Heating and cooling utilities savings	60
Table 5.6	TEHL for process hot streams.....	61
Table 5.7	TEHL for process cold streams.....	62
Table 5.8	Steam header information	63

	Page
Table 5.9	Source data for the GTL process..... 69
Table 5.10	Sink data for GTL process 69
Table 5.11	Comparison between a distillation column and a flash unit..... 72
Table 5.12	CO ₂ separation and recycling..... 73
Table 5.13	Estimation of CO ₂ separation cost 74
Table 5.14	Price for August 2008 75
Table 5.15	Costs of raw materials 75
Table 5.16	Costs of heating and cooling utilities 76
Table 5.17	Calculation of annual operating cost and savings with process integration 76
Table 5.18	Sales of GTL products..... 77
Table 5.19	TAC calculation for GTL plant..... 77
Table 5.20	Raw material cost for 4,300 BPD capacity 78
Table 5.21	Operating cost for the 4,300 BPD capacity..... 79
Table 5.22	TAC calculation for the different sizes 79

1 INTRODUCTION

1.1 Interest and Background

Natural gas is recognized as one of the cleanest and most abundant fossil fuels. With the growing global market for natural gas, it is important to identify effective methods for deploying the vital resource worldwide. In many cases, there is an economic incentive to ship the gas in liquid form which occupies much less volume than the gaseous form. In this regards two main approaches have been adopted: liquefaction leading to liquefied natural gas (LNG) and chemical conversion to convert gas to liquid (GTL). The key concept of a GTL process is to chemically convert the gas to longer-chain hydrocarbons that will typically be in the range of liquid transportation fuels. A leading GTL technology is the Fischer Tropsch (F-T) process.

It is beneficial to compare the key features of GTL and LNG. Table 1.1 lists (Patel, 2005) the main points of comparison between GTL and LNG, where BSCFD is set as billion standard cubic feet per day, BPD is barrels per day, MMTPA is million tones per year, bbl is barrels, CAPEX is capital expenditures. Carbon efficiency is defined as (carbon molecules in the final products)/ (carbon molecules in natural gas feed), and energy efficiency is set as (low heating value of liquid final products)/ (low heating value of natural gas), as indicated in that report. They produce quite different products for markets. The products of GTL range from gasoline and jet fuel to middle distillates. Different from LNG, middle distillates are the most popular products from GTL, and can be utilized as the feedstock to produce ethylene and propylene. Considering the cost for the process, GTL process will be prospective if the crude oil obtained diesel has a price higher than some limit. Affected by the recently price trend of crude oil, natural gas, and other facilities, the potential for the GTL process shows up (Steynberg and Dry, 2004).

This thesis follows the style of Bioresource Technology.

Table 1.1. Comparison between GTL and LNG (Patel, 2005)

	GTL	LNG
Product Capacity	1 BSCFD ~110,000 BPD ~5MMTPA	1 BSCFD ~280,000BPD ~7 MMTPA
CAPEX	\$2.2 billion (mostly in producing location)	\$2.4 billion (\$1.2 billion plant, \$0.8 billion ships, \$0.4 billion regasification)
Product value	\$ 24-27/bbl	\$16-19/bbl
Energy Efficiency	60%	85%
Carbon Efficiency	77%	85%

There are environmental advantages for using F-T based GTL technologies. These include low content of sulfur compounds and NO_x, coupled with the benefit of less aromatics left reducing the toxicity and the particulate matter generated when combustion. Focus also goes to the ability to diversify further to higher valued chemical products other than fuels, with a higher cetane number (70-80) allowing a superior performance for engine design (Hodge, 2003; Ijeomah, et al., 2008; Cooke, 2003; Jory, 2006; Kurevija, et al., 2007; Liu and You, 1999; Liu, et al., 2008; Rahmin, 2003; Weeden, et al., 2001; Wu, et al., 2007). Moreover, it tackles the problem of transportation of natural gas, and the products could be blended with refinery stock as superior diesel as an alternative way (Government of Qatar, 2007; Hall, 2005). The primary environmental advantages for GTL compared to refineries are illustrated in Fig. 1.1 (Rentech Inc., 2005).

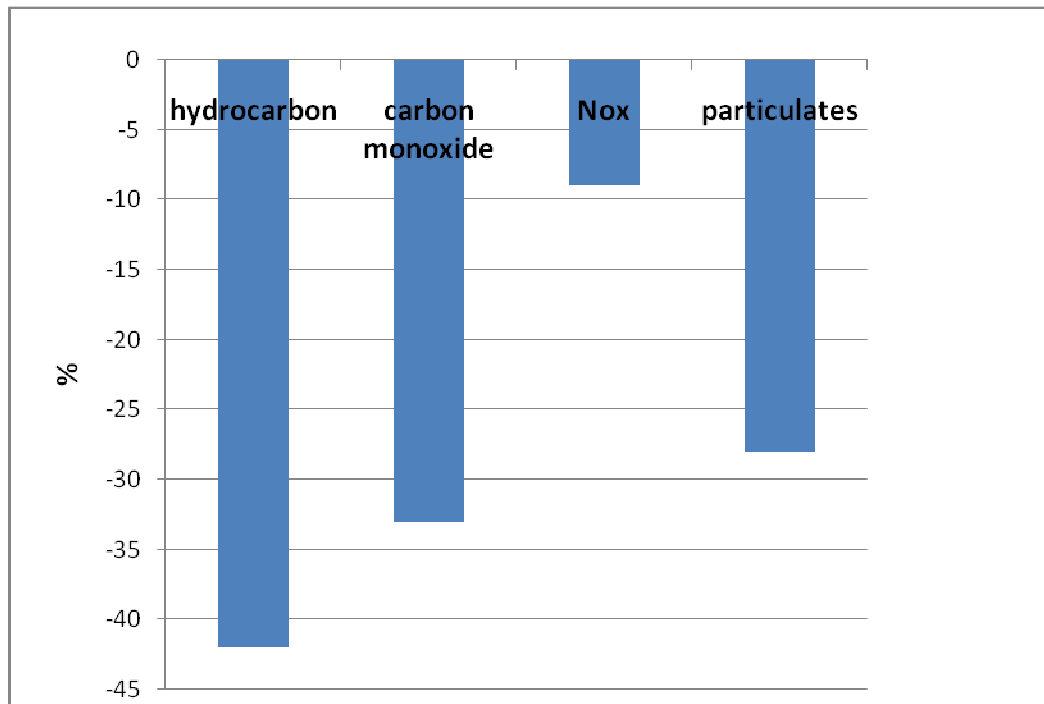


Figure 1.1. Environmental advantages of GTL processes compared to normal diesel (GTL emission reduction in percent based on normal diesel) (Rentech Inc., 2005)

1.2 Basic Process Steps

The GTL process is mainly comprised of three steps shown in Fig. 1.2. These are steam reforming of natural gas to produce syngas (CO and H₂), followed by F-T reaction, and finally upgrading of the products to cracking and hydro-processing units for the synthesis liquid hydrocarbons to yield products that meet the market specifications.

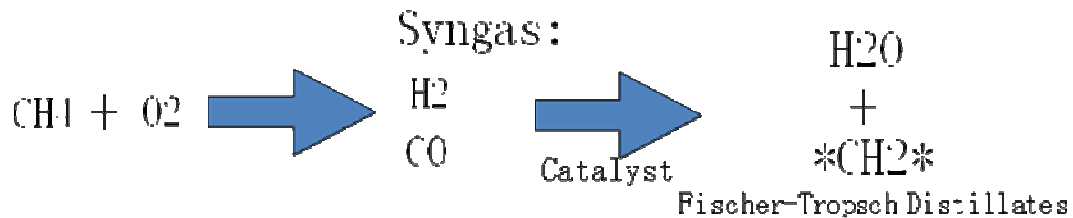


Figure 1.2. GTL process in chemistry

There are many design variables that complicate the F-T synthesis step (Steynberg and Dry, 2004). One of these is the catalyst since it will undergo changes during the reaction due to interaction with chemical species. The reactor performance is another important element. The gas velocity and the conversion rate can all be affected by the reactor diameter and height, as well as how the cooling system is installed. Of course, feed gas composition, reaction pressure and temperature should all be taken into account. The technology for the design comes with many optimization objectives and constraints. So the reaction rate and the product selectivity should be reconciled with the conversion rate and other considerations (Vessia, 2005; Vosloo, 2001).

To get an efficient process, many facets are generally dealt with falling into the categories of integrating and managing mass management and energy management (Steynberg and Dry, 2004). Often wasted gas from the main units is recycled back to conserve the resources. The same one is applied to the huge amount of waste water produced in the process. These involve various separation technologies associated with the manufacture of the F-T catalysts technologies. Another consideration is in the energy balance. In the whole process, there is a lot of energy consumed in various units. The distribution of cost investment for each unit in the process is illustrated in Fig. 1.3. It is important to point out that improving the energy efficiency is necessary both for environmental issues and economic considerations.

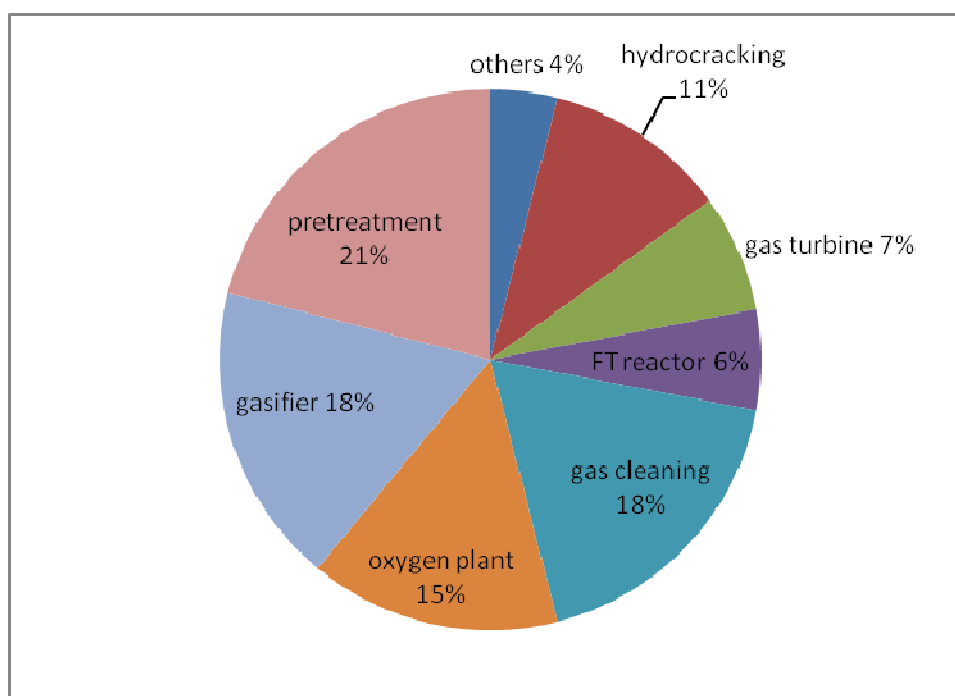
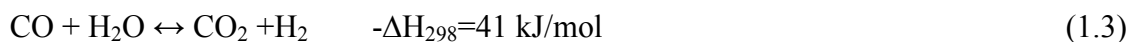
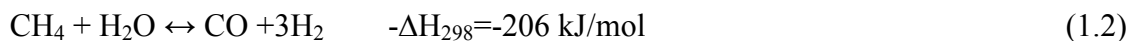


Figure 1.3. Energy consumption of each unit for GTL process (Tijmensen, et al., 2002)

1.2.1 Synthesis Gas Preparation

The first step is investigated by many researchers (e.g., Cao, et al., 2008; Nouri and Kaggerud, 2006; Repasky and Reader, 2004; Suehiro, et al., 2004; Wesenberg, 2006; Wilhelm, et al., 2001). The feedstock reacts with steam and oxygen to produce hydrogen, carbon monoxide and carbon dioxide. The technologies for producing syngas from natural gas involve: partial oxidation “POX”, catalytic steam methane reforming “SMR”, two-step reforming, autothermal reforming ATR, and heat exchange reforming. The choice of the reactor is determined by balancing between the characteristics of each one. SMR doesn’t require oxygen and high temperature, but it produces much higher hydrogen to CO ratio than needed. POX could allow absence of catalyst and thus lower CO₂ content, but it requires oxygen and high operating temperature causing soot formation that’s hard to handle. ATR, known as endothermic syngas reforming reactions automatically happening by virtue of the internal heat brought in by oxidation of a portion of the feed hydrocarbons, has the most favorable H₂/CO ratio, but it needs

oxygen to proceed and has limited commercial experience. Heat exchange for reforming can use compact equipment and introduces flexibility to application, but in some cases it must be coupled with other syngas producing techniques to achieve the job. Oxygen-blown reforming has received more attention over air-blown reforming in the low air compression power demands, high thermal efficiency, the ability to recycle F-T tail gas, and the smaller downstream equipment sizes mission (Repasky and Reader, 2004). Also, ATR shows up in many commercial processes due to the ability to handle large scale scenarios. The reactions carried on in the ATR can be expressed as follows (Yagi, et al., 2005; Suehiro, et al., 2004):



The H₂/CO ratio is subject to adjustment by controlling some factors including the flowrate of CO₂ and use of steam. While recycling CO₂, and removing H₂ will decrease ratio, increasing steam would yield opposite effect (Lu and Lee, 2007).

The major requirement for the feed is composition of carbon. In this regard, the feed does not need to be natural gas, since it may range from coal to biomass, etc. The clean nature of natural gas makes it feasible to use expensive catalyst, although the cost from coal to syngas will be much lower (Cornelissen and Hirs, 1998; Steynberg and Dry, 2004). Considering the emissions from this step, GTL will take the advantage not only in the low content of sulfur and NO_x, but also in the soot particles. In this step, the oxygen is consumed almost completely, and the excess unconverted gas is either burned to produce more heat and power or recycled to the reformer. There is potential benefit from carbon dioxide removal both in reducing the emissions and in the improving the productivity.

Tam (Tam, et al., 2001; Vessia, 2005) introduces a method for high pressure carbon dioxide separation process for IGCC (integrated gasification combined cycle) plants,

comparing the economic cost and benefit between the old configuration and this new continued development of the process, stating the cost reducing advantage of the new invented process. In the process of steam reforming, combined steam and carbon dioxide reforming of methane (CSCRM) is catching eyes from researchers. This presents disadvantages in controlling the syngas usage ratio and the energy consumption.

1.2.2 Fischer-Tropsch Synthesis

The Fischer-Tropsch (F-T) reaction is highly exothermic, which is a significant characteristic, thus influencing the efficiency of the whole process. The kinetic process can be expressed by the following equation (Suehiro, et al., 2004)



The F-T process produces olefins, alcohols, acids, oxygenates and paraffins of different length. The products distribution follows Anderson-Schulz-Flory (ASF) (Kuipers, et al., 1996) distribution as long as there is constant probability of chain growth factor, with the function being $W_n/n = (1-\alpha)^2 \alpha^{n-1}$ where W_n is the mass fraction of the hydrocarbons containing n carbon molecules and α is the chain growth probability of the molecules to continue reacting to form longer chains, exponential function described in Fig. 1.4. A typical F-T product distribution is shown in Table 1.2.

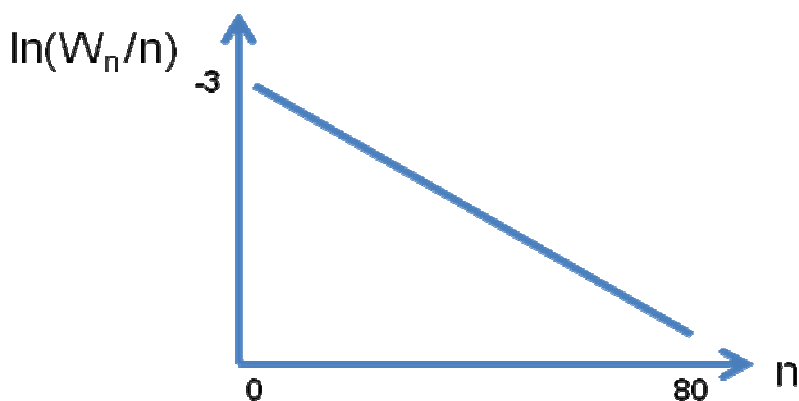


Figure 1.4. ASF distribution of GTL products with log scheme

Table 1.2. Example of a pilot F-T product distribution (Steynberg and Dry, 2004)

Catalyst	Cobalt	Iron	Iron
Reactor type	Slurry	Fluidized	Slurry
Temperature °C	220	340	240
% Selectivities (C atom basis)			
CH ₄	5	8	4
C ₂ H ₄	0.05	4	0.5
C ₂ H ₆	1	3	1
C ₃ H ₆	2	11	2.5
C ₃ H ₈	1	2	0.5
C ₄ H ₈	2	9	3
C ₄ H ₁₀	1	1	1
C ₅ -C ₆	8	16	7
C ₇ -160 °C	11	20	9
160 °C-350 °C	22	16	17.5
+350 °C	46	5	50
Total H ₂ O soluble oxygenates	1	5	4
ASF α value	0.92	0.7	0.95

Commercial scale F-T reactors (e.g., Davis, 2002; Davis, 2005; Elbashir and Roberts, 2005; Krishna and van Baten, 2003; Krishna and Sie, 2000; Krishna, et al., 2000a; Sie and Krishna, 1999; Steynberg, et al., 1999) include multi-tubular fixed bed reactors, fixed fluidized bed reactors, circulating fluidized bed reactors, and fixed slurry bed reactors (see Fig. 1.5). Fixed bed reactors place catalyst inside the tubes whereby surface the reactions take place, while cooling medium on the shell sides. Circulating fluidized bed reactors recycle part of the products from the reaction through outside tubes to assist the internal cooling system. In the slurry bed reactors the catalyst is suspended in the liquid wax medium itself. F-T reactor technologies are classified as low temperature process (LTFT) or high temperature process (HTFT). LTFT process normally ranges between 200-240 °C while HTFT process ranges between 300-350 °C (e.g., Krishna, et al., 2000b; Krishna, et al., 2001a; Sie and Krishna, 1999; Elbashir and Roberts, 2005). Most of HTFT processes conducted in absence of liquid phase. Two most important

design factors are temperature control and heat removal for large-scale commercial F-T reactors when considering product selectivity and catalyst lifetime. Features affecting choice of reactors also include gas-solid separation, catalyst settling, scaling-up aspects, mass transfer, heat transfer, recycle effect, and diffusion problems. F-T synthesis depends on the feedstock and the desired products. The features for each type of reactor are shown in Table 1.3.

Catalyst role in FTS reaction is discussed good details in several reviews studies (e.g., Brumby, et al., 2005; Dry, 2003). Besides the comparing catalyst efficiency and other economic issues related to process operating costs, H₂ to CO ratio is another important parameter to study. For cobalt- catalysts H₂ to CO ratio is suppose to be around 1.8-2.1, while for iron catalysts H₂ to CO ratio is way below 1 as a favor for water gas shift reaction (Koo, et al., 2008a; Steynberg, et al., 1999). Iron catalysts are better suited to use with coal derived synthesis gas because cobalt catalysts are more expensive and it is difficult to prevent coal derived catalyst poisons.

In the case of different temperature reactions, HTFT process is still competitive in the higher value products it can produce. Moreover, at higher temperatures, it is also convenient to achieve high conversions. However, the LTFT process is also capable of providing higher value products such as base oils and detergent feedstocks with further processing. So to achieve large quantities of products in a future view, LTFT will be a better choice (Steynberg and Dry, 2004).

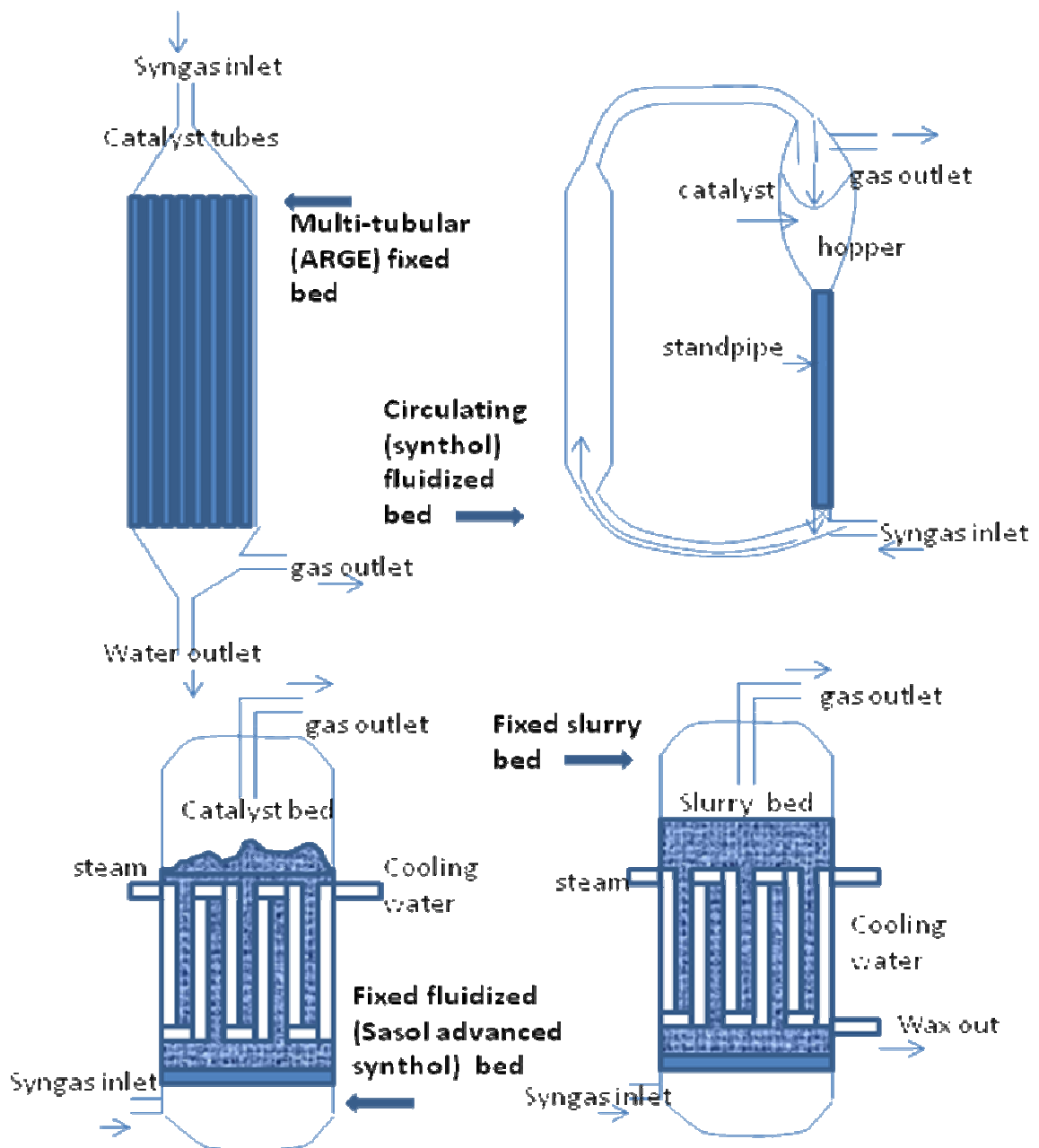


Figure 1.5. F-T reactors (Spath and Dayton, 2003)

Table 1.3. Features for each F-T reactor (Dry, 1981; Steynberg and Dry, 2004)

Reactor bed type	fixed	slurry	Fluidized	slurry
Catalyst type	Precipitated		Fused	
Particle size	2.5 mm	40-150 μm	<70 μm	< 40 μm
Fe loaded (kg)	2.7	0.8	4.2	1.0
Expanded bed height (m)	3.8	3.8	2.0	3.8
Average bed temperature ($^{\circ}\text{C}$)	230	236	323	324
Recycle to fresh feed ratio	1.9	1.9	2.0	2.0
Total gas linear velocity (cm/s)	36	36	45	45
Fresh feed conversion (%)				
CO +H ₂	46	49		
CO + CO ₂			93	79
Selectivity (C atom basis)				
methane	7	5	12	12
gasoline	14	15	43	42
Hard wax (BP>500 $^{\circ}\text{C}$)	27	31	0	0

1.2.3 Product Upgrading

Separation is typically the way to tackle the products with many phases. Pressure requirements should be met to facilitate the atmospheric storage. First light gases are separated. Oxygenated compounds are usually removed from the liquid for the ease of later processing. Then, through fractionation and extractive distillation olefins could be removed from the straight liquid products. They are either oligomerised, alkylated or hydroformylated to produce desired products or blended with other liquid products for the mixing use. The other products are generally converted into naphtha and diesel by the means of hydrogenation step and fractionated. The naphtha can be further processed to gasoline. For LTFT processes with cobalt catalyst only hydroprocessing and

separation are employed since the olefin content is low (Steynberg and Dry, 2004; Perry and Green, 1984; Maiti, et al., 2001).

Usually, the produced diesel is blended with special chemicals to enhance stability. At the same time, other methods may be used to improve properties such as lubricity. Chemical conversion is one method involving hydro-isomerisation, in which straight chain hydrocarbons are changed to branched ones for improving cold flow properties. While long chain hydrocarbons have two ways to go. One is hydrocracked to further provide naphtha. Alternative one is hydroprocessed to high quality lubricant base oils. To get further cuts or fractions, vacuum or short path distillation is used to produce special demanded wax or products (Steynberg and Dry, 2004).

In light of the increasing demand for diesel for transportation and industrial uses, producing diesel mainly from GTL process is a good choice, especially this diesel is very low in sulfur content. Thus, wax could be cracked with certain selectivity to diesel with the help of special catalysts, and produced naphtha is another resort to get diesel through various processes.

The plant scale generally depends on whether the latter processes are justified. Although the LPG with C₃ to C₄ paraffins takes little place in the whole products, it shouldn't be looked down for the significant higher prices. It is recovered directly from the vapor product of the F-T reactor. They can be further produced to plastics or cracked to olefins. Small fractions of oxygenates are dissolved in the reaction water and by distillation from the bulk water they can be processed to a variety of chemical ranges (Steynberg and Dry, 2004).

1.3 Historical Development

The research and development (Freerks, 2003) of GTL application has come through a long history. The first industrial F-T reactor was constructed as a fixed bed reactor by

Franz Fischer and Hans Tropsch in 1935 trying to produce liquid fuels from gas and coals. Later, the successful pilot plant experience at Oberhausen-Holten acted as a major milestone in F-T synthesis. World War II behaved as an initiator to scale up the process when pushing for a petroleum boom. At that time all the plants were atmospheric pressure operated and used low temperature technology. In 1940s, American companies began to construct plants of this technique, mainly with HTFT. And HTFT solidified basis for the GTL plant currently in operation in Africa. In 1955 circulating fluidized bed (CFB) reactor found its application in Sasol and went along as an attractive F-T reactor (Steynberg and Dry, 2004; Chedid, et al., 2007).

Shell Malaysia tested its commercial application on GTL in 1993 at Bintulu plant, converting 140 million cubic feet of gas into 14,700 barrels of liquids per day by employing Shell middle distillate synthesis (SMDS) technology. The SMDS diesel fraction is known as ultra-clean fuel that protects the engine injection system. After that Shell introduced new generation of the multitubular F-T reactors to its Pearl GTL project in Qatar of capacity about 140,000 bbl/d (this is the largest energy project so far around Qatar). A process flowsheet for Sasolburg is shown in Fig. 1.6. Another big project is Oryx GTL plant using internally cooling slurry phase distillate process (SPD), acquiring 34,000 bbl/d production (Crook, 2007; Dry, 1982; GTL Task Force Department, 2001; Halstead, 2006; Hoek, 2005; Smith and Klosed, 2001; Steynberg and Dry, 2004).

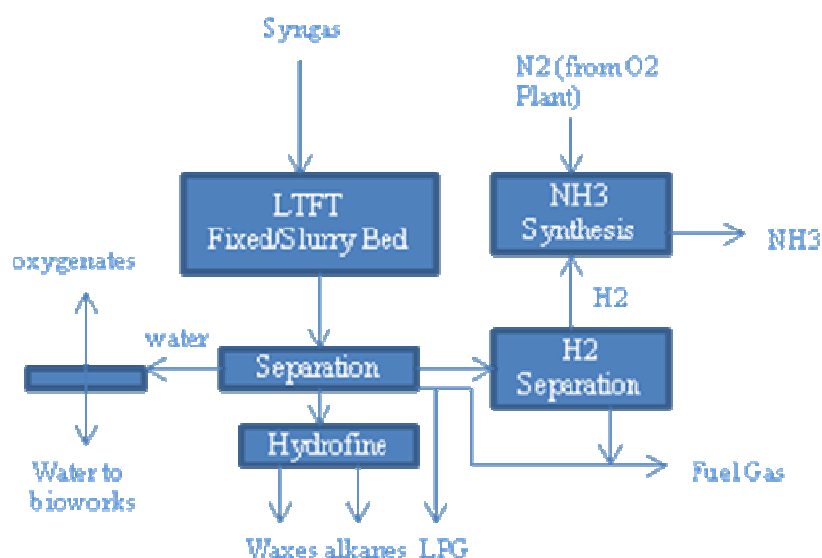


Figure 1.6. Sasolburg GTL process (Steynberg and Dry, 2004)

Here is a summary of some commercial development in GTL applications (Rahmim, 2003) listed in Table 1.4.

Table 1.4. List of GTL commercial development (Rahmim, 2003)

Sasol Chevron	<ul style="list-style-type: none"> ● Developed new slurry-phase distillate process (SSPD) employing cobalt catalyst in 1990s ● South African plants used Lurgi coal gasifiers for syngas production and multitubular fixed-bed and fluidized-bed reactors for the F-T step ● Combined partial oxidation process for syngas production with Chevron product upgrading technology ● Designed F-T reactors including circulating fluid bed (Synthol), multitubular fixed-bed with internal cooling (Arge), non-circulating fluid bed reactors (SAS), and SSPD ● Had contracts with Qatar (Sasol ConocoPhillips)
---------------	---

Table 1.4. Continued

Shell	<ul style="list-style-type: none"> ● Manufactured partial oxidation based syngas formation unit ● Used Shell Middle distillates synthesis reactors (SMDS) ● Expanded Bintulu due to explosion of air separation unit in 1997
ExxonMobil	<ul style="list-style-type: none"> ● Developed AGC 21 technology that employs catalytic partial oxidation for syngas production, slurry-phase bubble-column F-T reactor for chain growth, hydro-isomerization to produce wax ● Used Cobalt and Ruthenium-based catalysts ● Operated 200 BPD GTL pilot plant in Baton Rouge since 1996
ConocoPhillips	<ul style="list-style-type: none"> ● Used catalytic partial oxidation for syngas production step ● Developed F-T catalyst and designed high efficiency reactor ● Had Qatar joint contract with Sasol
BP	<ul style="list-style-type: none"> ● Employed compact steam reformer for syngas production (1/40th of conventional size) ● Used fixed bed F-T reactor with more efficient catalyst ● Employed wax hydrocracking for upgrading ● Alaska plant in start up (1Q2003)
Syntroleum	<ul style="list-style-type: none"> ● Used nitrogen in air to remove heat from ATR (autothermal reformer) in syngas production ● Rejected air separation unit ● Cost less than commercial technologies ● Employed fixed-bed or fluidized-bed F-T reactor with cobalt-based catalyst ● Used hydrocracking for upgrading
Rentech ¹	<ul style="list-style-type: none"> ● Had access to the Texaco gasifier ● Combined partial oxidation with SMR for heat balance ● Employed slurry phase reactor and iron-based catalyst for F-T reaction

¹ Rentech GTL information is available at <http://www.rentechinc.com>.

1.4 Literature Review

Lu (Lu and Lee, 2007) has shown that the feed gas composition to the F-T synthesis plays a major role in determining the chain length and the hydrocarbon product distribution. Several studies that utilized data collected from pilot plant, lab experiment, and semi-simulation looked at influence of syngas composition on product yields, energy efficiency, and carbon utilization (e.g., Suehiro, et al., 2004; Reddy and Basu, 2007). They suggested by later recycling process to adjust H₂:CO ratio, the carbon efficiency for the process will increase to 50% based on the case in that paper. CO₂ function was also examined and only a diluting role was found under current commercial slurry phase F-T process.

Another paper indicates (Iandoli and Kjelstrup, 2007) that heat and power exergy is related in some way to operation cost. It's better to fully utilize the heat and find a balance between power consumption and work produced. Simulation work has been done based on slurry phase process using cobalt based catalyst focusing on the efficiency of both HTFT and LTFT. Air separation unit is indicated to be a major power consumption unit and heat released from F-T reactor can be a supplement to it. By controlling CO₂ content waste exergy will be adjusted.

Issues with reactor modeling have been addressed by some researchers (e.g., Hao, et al., 2008; Khoshnoodi, 1997; Levenspiel, 2002; Sehabiague, et al, 2008). Using a rigorous calculation of vapor-liquid equilibrium Quasi-steady-state model was proposed to be suitable to the transient simulation considering two chain propagation mechanisms (e.g., Ahon, et al., 2005; Khoshnoodi, 1997; Wang, 2004; Zhang and Zhu, 2000). Results showed that the hydrocarbon product distribution could be explained by including both olefin readsorption and the propagation mechanisms. Process simulation analysis has been conducted on the once-through concept and recycle model to investigate the carbon efficiency and the selectivity towards C₅₊. Other simulation comparisons have been tested to evaluate different property method applicable in the process (e.g., Ahon, et al.,

2005; Hao, et al., 2008; Soterious and Ignacio, 1983; Wang, 2004; Zhang and Zhu, 2000).

A new GTL process is proposed (e.g., Jaramillo, 2007; Larsson, 2007; Suehiro, et al., 2004) to be candidate in natural gas utilization mainly focusing on reducing green house gas emissions although GTL is quite low in other emission discharges. Energy system aspects of this process are summarized with an attempt to get an overview of the pathway, figuring out the economic issues with the emissions.

A full product life cycle assessment was conducted on GTL process by three joint companies (Five Winds International Inc., 2004). Result showed that waste released from GTL is dramatically reduced compared with other diesel production processes. Fig. 1.7 shows the CO₂ distribution from each unit in the GTL process calculated from Iandoli's paper. By constructing a model to research economy influence, they concluded GTL industry will bring significant benefits to government and society, conceiving a very promising industry in market.

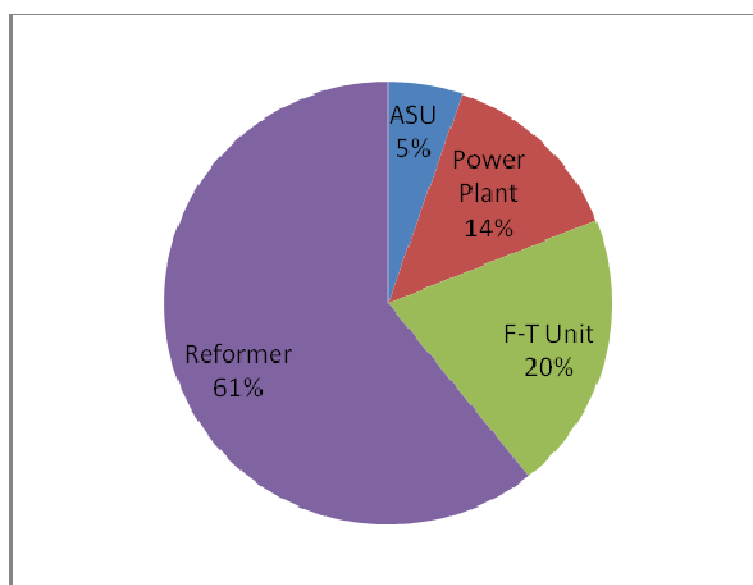


Figure 1.7. CO₂ from each unit (Iandoli and Kjelstrup, 2007)

1.5 Relevant Features

1.5.1 F-T Reactor Design

There are many design and scale-up problems relating with the F-T reactor. These problems have several features. First, the process should consider the high pressure operating conditions. Second, the highly exothermic reaction makes the reactor need enormous cooling systems to remove the heat generated in the process. Third, the scale up and flow rate determine the reactor diameter and heights to satisfy the production requirements. Further focus is needed for mass and heat transfer, residence time in the reactor forms a basis for the simulation and integration of the process (Krishna, et al., 1996; Krishna, et al., 2001b). The comparisons of these reactors are summarized in Table 1.5 (Fox, 1990; Jarosch, et al., 2005; Maretto, 2001; Maretto, et al., 2001; Saxena, 1995; Sie and Krishna, 1999).

Table 1.5. Comparison between different types of F-T reactors

Reactor	Gas-solid fluidized reactor	Multitubular trickle-bed	Slurry bubble column
Products	Applicable gasoline	Heavier products	Heavier products
Application	Growth chance parameter less than 0.7	Safe for straightforward scale up	Best for large capacity

Here is some illustration (Steynberg, et al., 1999) of comparison, for example, the SAS reactor and CFB reactor. They pointed out that SAS (Sasol advanced synthol) reactor makes use of the important term of bed voidage, which indicates the amount of catalyst a given reactor volume can handle, affecting the conversion of the reaction product. The function of the reactor can be well understood by taking a look at the reactor scheme that consists of gas distributor to carry up syngas stream, the fluidized bed for catalyst to react, cooling coils dispersed throughout the bed, and cyclones to separate entrained

catalyst from the product. The system could also be modeled based on the information related to process dynamics and catalyst kinetic and selectivity performance.

CFB (circulated fixed bed) reactor is composed of fast fluidized bed, settling hopper, standpipe and slide valve. In the system catalyst flows down the standpipe with reaction flow and builds up the pressure along it until reaching the valve. After the catalyst goes through the valve, it meets with high velocity synthesis gas and thus is carried up vertically along the bed section. In the hopper the gas leaves the system and at the same time separated from catalyst with the help of cyclones. Then the standpipe protects the reaction gas against continuing passing through the reactor, while maintaining necessary pressure recovery to hold up the catalyst flow to guarantee sufficient yield (Steynberg, et al., 1999).

Taking the two reactors into consideration, catalyst contacting gas quantity is about twice for SAS than that of CFB, since half of catalyst is in the standpipe zone for CFB, on the basis of the same amount of catalyst present in both reactors. Another significant factor is the energy efficiency which benefits more from the cooling coils from SAS, as well as the larger cooling area installed in SAS due to the constraints placed by the maximum velocity and pressure balance requirements in CFB. Due to these benefits, SAS has fewer demands for external heat exchangers and pumps, resulting in further economy scale advantages. Other faces needed to consider are the catalyst consumption which is extremely decreased in SAS, and the increased steam production resulted from the power management, lowering the cost pretty much. Catalyst consumption is the term to describe that in the process there will be free carbon produced favoring CFB, which will considerably dilutes the catalyst in the reactor. The increased product conversion leads to the decreased cost for recycling tailgas (Steynberg, et al., 1999).

Wang (Wang, et al., 2003) constructed a model to predict the heterogeneous fixed bed F-T reactors taking into account the catalyst pores filled with liquid wax. They reported

that it outperformed other models. This one is very detailed in the selectivity of the catalyst. To report the selectivity, the usage ratio, recycle performance and cooling effect are investigated. Others (Iliuta, et al., 1999) take a view on the trickle-bed reactor's mass transfer and fluid dynamics characteristics, on the basis of investigating flow regime database.

Since the products consist of gases, liquids, and solids, taking place in three phase system, the efficient mass transfer attracts significant attention (Sie and Krishna, 1999). Commercial scale reactors are mostly developed in World War II, which present lots of limitations for pressure drop and capacity aspects. Later large scale reactors are developed. Multitubular fixed bed reactor, fluidized bed and slurry bed reactors are the main commercial reactors. The features of fluidized bed reactors are good heat transfer performance free from diffusion limitations, although the fluidized bed reactors inevitably get products to agglomerate around the surface of the catalysts. The pore diffusion limitations are evident in fixed bed reactors making the reaction rate quite low, in addition to the affect from heat transfer problems and pressure drop problems. There are two main regimes for slurry phase reactors, the bubbly flow regime and the churn turbulent regime. To achieve high product output, the gas velocity need be as high as 0.4 m/s, which is within the churn turbulent regime. Besides the excellent heat transfer feature for the slurry reactor, effective mass transfer also gives rise to the application in homogeneous regime of this reactor (Sie and Krishna, 1999).

For economic reasons F-T conversions are better carried out in large scale plants and therefore scaling up is an important selection factor to consider. To guarantee the success of the scale up of the reactors, careful sights should be given to the aspects of gas hold up, interphase mass transfer and dense phase backmixing as listed by (e.g., Krishna and Sie, 2000; Sie and Krishna, 1999; Urseanu, et al., 2003; Vandu and Krishna, 2004). As listed previously, the slurry bubble column reactor is an ideal reactor type for large scale plants.

Most of the design parameters are correlated (Steynberg and Dry, 2004). For example, heat transfer will be influenced by bubble rise velocity, because heat transfer is determined by the formation rate of the liquid film on the tube, while the formation rate is under bubble velocity control. Moreover, the gas hold-up and axial dispersion are also dictated by the velocity, and they can affect the distribution of bubble sizes along the reaction section. On the basis of maximizing the reactor dimensions (Steynberg and Dry, 2004), it is much less expensive to add reactor height rather than reactor diameter. The consideration facets are placed on economic design, fabrication constraints, and effective transport ways. Another approach (Steynberg and Dry, 2004) under consideration is the use of reactors in series. This allows water removal between stages and increases the partial pressure for the syngas. Accompanying it is the reduced recycle ratio and reactor volume, which are both welcomed. However, research is going on to find out whether these effective advantages will overcome the complexity from the series configuration for the reactors.

1.5.2 F-T Catalysts

Typically the F-T catalyst takes use of ceramic to act as support, base metal to behave as the active metal, and precious metal (e.g., platinum, ruthenium) to promote the catalytic reaction (Steynberg and Dry, 2004). Concerning the preparation (Steynberg, et al., 1999) of the catalyst for the F-T reaction, catalyst parameters like mechanical strength and surface area play an important role, depending on the mole ratio, fusion, distributing variables.

Only four metals, Fe, Co, Ni and Ru (Table 1.6) are applicable for their activity in the reaction. The most active one is Ruthenium, but the cost is too high for large capacity production. Nickel is not practical either, for the reason that it will form volatile material during the operation conditions of F-T and get lost. The above reason leaves only Fe and Co to be applied in the large plant production. Cobalt is more active than Fe, however it is expensive. So in choosing the catalyst, the special conditions and target products of F-

T reaction determine the application. Iron is good in HTFT reactors at catalyzing high value linear alkanes, so iron can be chosen for producing this type of products (Steynberg and Dry, 2004; Song and Sayari, 1996).

Koo (Koo, et al., 2008a; Koo, et al., 2008b) listed the criteria for choosing F-T catalyst considering the molecular adsorption and formation effect to overcome the disadvantages listed above. They also introduce an effective and stable nano sized catalyst for the F-T reaction. It also tells the way to adjusting the usage ratio other than controlling the feed steam to gas ratio, by looking into the agglomeration, dispersion and activity of the different types of catalyst.

To increase the economic use cycle of the catalyst, recycling the catalyst is a mandatory way. Brumby (Brumby, et al., 2005) discusses some of the challenges and the economical concerns when considering catalyst recycling strategy. In their paper the demand, supply and prices of the most used catalysts for the oil refining process were given. To facilitate economically valid recycling process they have combined recycling of the base metal with the recycling of the precious metal, weighing two potential methods: precipitation or pyrometallurgical method.

Table 1.6. The features for each catalyst (Steynberg and Dry, 2004)

Catalyst	Pressure (bar)	Conversion %	Relative production
Co	60	47	109
Co	30	86	100
Co	3	99	12
Fe	30	37	43
Fe	60	37	86
Fe (5x more active)	30	68	79
Fe (5x more active)	60	68	158

The following lists factors associated with lowering activity for F-T catalyst (Steynberg and Dry, 2004)

- Fouling in catalyst pores will bring diffusion problems for catalyst.
- Elemental carbon depositing on the surface of catalyst, will cause less contacting area for catalyst and reactant.
- Poisons from feed gas in the form of H₂S or sulphur compounds will cause the catalyst less active.
- Due to hydrothermal sintering, catalyst will be less active.
- Due to oxidation, the catalyst metal will become inactive crystals.

In the presence of cobalt catalyst, heat removal is a serious issue to consider. If the heat exchange is not effective enough, large amount of methane will be produced. Heat removal is also important for both catalysts since improper temperatures will result in formation of light hydrocarbons and coke that may lead to deactivation of active sites on catalysts (Steynberg and Dry, 2004).

1.5.3 F-T Products Processing

The target chemicals and fuels production range dominates the specifications and configuration for the refining technologies. So in designing the refining processes, the chemical range split should be taken into consideration. An example is shown in Table 1.7 about the distillation range. On serving the refining options for different cuts of products, the specific properties of each desired products are considered for specific approach to be applied.

Table 1.7. Distillation range for LTFT synthesis crude (or syncrude) fractions (Steynberg and Dry, 2004)

Distillation range	F-T condensate % vol	F-T Wax % vol
C ₅ -160 °C	44	3
160-270 °C	43	4
270-370 °C	13	25
370-500 °C	-	40
>500 °C	-	28

Based on the previous discussions for different F-T temperature products and approach choosing, upgrading can be divided into HTFT products upgrading and LTFT products upgrading (Steynberg and Dry, 2004). For HTFT upgrading, here are some common attributes of the products that can impact the refining process (Steynberg and Dry, 2004):

- Products head toward light hydrocarbons, following ASF distribution.
- Products are mostly linear.
- They show high percent of olefinic products.
- They are low in aromatics and naphthenics.
- Products contain certain amount of short chain oxygenates.

So in exploiting the olefin abundant products, the following refining processes are required (Steynberg and Dry, 2004)

- Oligomerization can be employed to convert light products to higher carbon materials, since products head toward light hydrocarbons.
- Isomerisation is also recommended to improve the octane number and the density.
- Hydrogenation can be conducted to remove excess oxygenates, olefins, etc.

It will be noted that thermal cracking and alkylation are not involved in the process. But they will be included if the products have longer chain materials. To summarize, the following factors are listed to illustrate the exact principal for the choosing approach to

upgrading configuration, taking into account the plant size, capital constraints, and product pricing, etc (Steynberg and Dry, 2004).

- The first principle is to minimize waste to guarantee most products.
- Paraffin products should be upgraded.
- Target should be placed for higher value products.

The LTFT products are generally suited to process to middle distillates with naphtha as the main co-product. Diesel is the most ideal middle distillate product with the suitable market prices. To exploit middle distillate products, heavy F-T paraffinic wax can be hydrocracked and light olefins can be oligomerised. The remaining naphthas are used as feedstocks for steam crackers. It is obviously applicable to integrate LTFT with HTFT in order to shift the products carbon number for better diesel value (Steynberg and Dry, 2004).

The selection of the configurations from hydroprocess, cracking, isomerize methods are in the same fashion with the choosing in HTFT as long as the desired products are targeted.

1.5.4 Chemical Concepts

To obtain a high degree of flexibility regarding the type of products and the carbon range, factors (e.g., selectivity, conversion, chain growth factor) can be manipulated with chain growth factor as an essential one. When probability of chain growth is determined, the selectivity is determined. These factors (e.g., chain growth probability) can vary in the reaction temperature, the choice of catalyst, the syngas usage ratio and the partial pressures of the reactant (Adegoke, 2006; Steynberg and Dry, 2004; Van der Laan, 1999).

First, temperatures should be considered. Desorption of the growing surface can terminate the chain growth reaction. It's endothermic. So processes with higher

temperatures will favor the desorption. By increasing temperatures the spectra can be shifted to lower carbon number products (Steynberg and Dry, 2004).

For the same thermodynamic reason, as the temperature increases the degree of chain branching increases. The hydrocarbon product distribution will produce lower alcohols and acids and at the same time the ratio of alkenes to alkanes will decrease, since higher temperature accelerates hydrogenating (Steynberg and Dry, 2004).

Irrespective of temperatures, catalyst surface coverage is also an important factor in determine F-T selectivity and conversion. It is stated that desorption and hydrogenation will lead to termination of chain growth reaction. On the basis that higher CO ratio can lead to higher catalyst surface coverage, higher CO will increase chain growth probability. Therefore, it's not hard to argue that increasing the H₂/CO ratio, chain termination is easier to happen, and in that manner much lower molecular hydrocarbons will be produced (Steynberg and Dry, 2004).

WGS (water gas shift) reaction often accompanies the F-T reaction. When cobalt acts as catalyst the extent is usually negligible, unlike the case for iron catalyst. When iron catalyst is present, WGS reaction works toward reverse direction, which consumes CO₂ and further promotes the F-T reaction (Steynberg and Dry, 2004). So it's possible to reduce the CO₂ emissions from the GTL process.

2 PROBLEM STATEMENT

Given a GTL process with certain units and feedstock specifications, it is desired to develop a techno-economic analysis of the process and to reduce its cost and enhance its energy efficiency.

The questions to be addressed follow as:

- How can the base-case process be simulated and analyzed?
- How should the process be retrofitted to reduce the cost?
- What are opportunities for energy and mass integration? What are the targets for performance? And how to achieve these targets?

To address the aforementioned problem, the following tasks will be undertaken:

- Development of a base-case design of gas to liquid process
- Techno-economic evaluation of the GTL production processes
- Mass and heat integration of the GTL processes

The schematic representation of the problem statement is shown in Fig. 2.1.

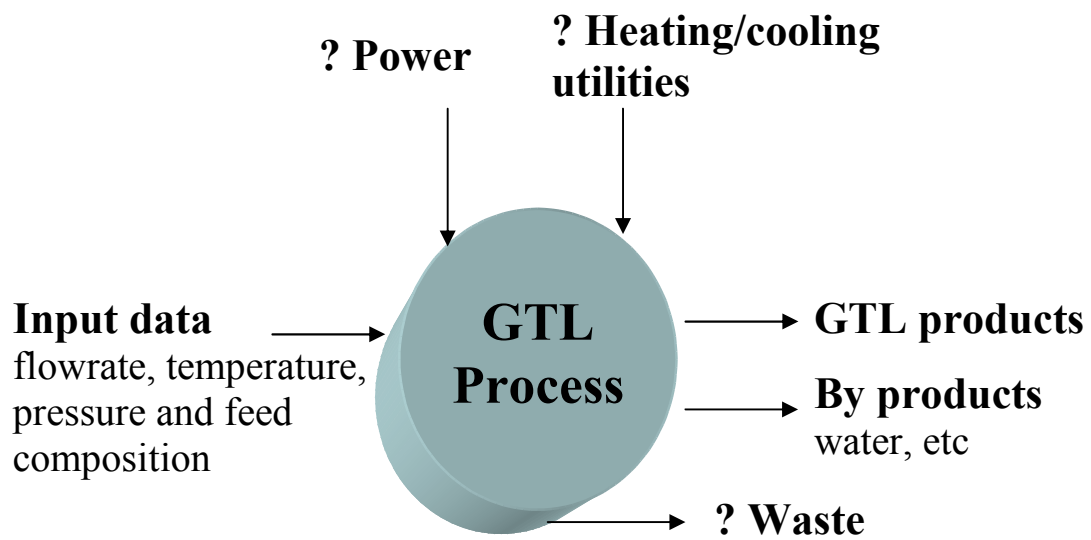


Figure 2.1. Schematic representation of the problem statement

3 METHODOLOGY AND APPROACH

3.1 Overview of the Design Approach

After thorough examination on the base case GTL process and the problem to be solved, description of the design approach and the methodology is illustrated here. The design approach is intended to evaluate and enhance the performance of the GTL process. Special attention is given to improve the energy usage of the process. This is an important factor given the substantial energy usage in GTL production. In this regard, the activities (Fig. 3.1) are undertaken to address the problem aimed at reducing energy consumption and enhancing the process performance:

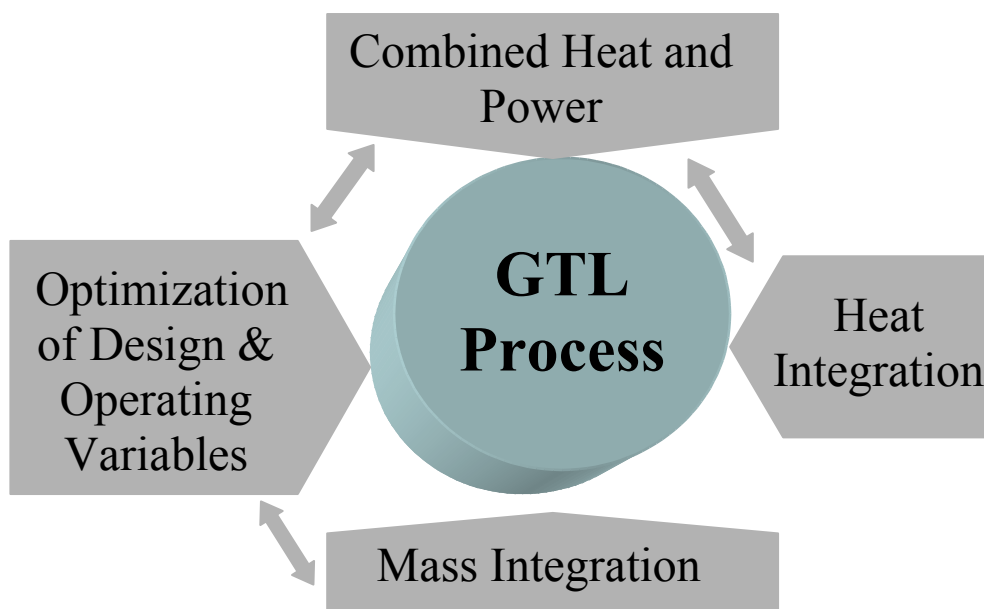


Figure 3.1. Overview of the GTL process analysis

Fig. 3.2 illustrates a hierarchical approach to optimize the GTL system. It consists of a sequence of interlinked steps that analyze and integrate the process.

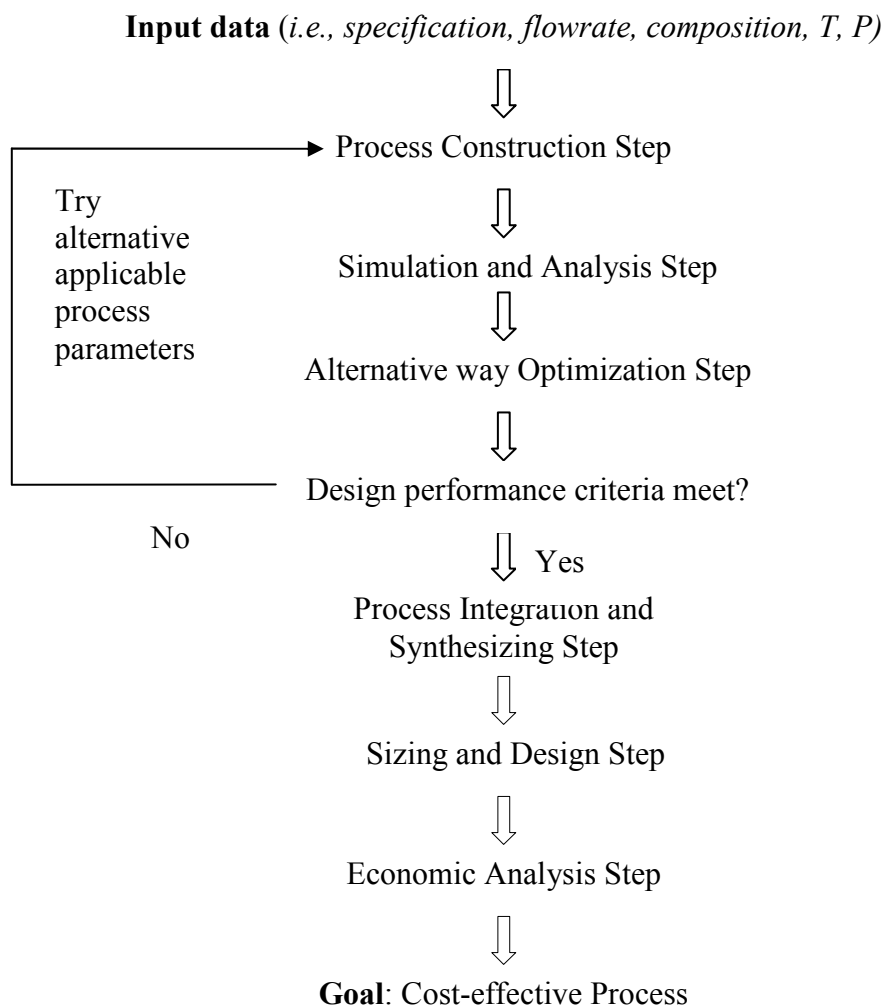


Figure 3.2. Hierarchical design approach

For each step, detailed approaches are planned here to facilitate the implementation.

- Formulate a typical GTL flowsheet from literature data and develop process

alternatives (e.g., H₂/CO).

- Run ASPEN Plus simulation, perform design specifications and sensitivity analysis, and optimize operating conditions (e.g, temperatures and pressures).
- Apply thermal pinch analysis and synthesize a network of heat exchangers using MILP (mixed integer linear programming) formulation. Apply mass integration to the tail gas compositions as well.
- Specify utilities cost and use ICARUS cost evaluator for evaluation of fixed and operating costs.
- Conduct analysis to the heat and power integration.

Here is the description of the schematic representation of the sequential steps. First, data and variables are selected based on literature review to create a base-case process flowsheet with basic information. After simulation of the synthesized flowsheet with a computer-aided simulation package (ASPEN Plus), specific characteristics of the key pieces of equipment and streams are determined. Alternative ways are developed and sensitivity analysis is carried out to explore the impact of varying the initial design specification. The abovementioned steps should be repeated if the results obtained from these efforts do not meet required specifications of the process. To reduce heating and cooling utilities, heat integration using pinch analysis is conducted to conserve the process energy. The pinch analysis determines the minimum heating and cooling utilities. In order to reach these targets, a mixed integer linear program (MILP) is developed and solved using the optimization software LINGO. Additionally, mass integration is carried out to conserve mass resources. The recycling of the catalyst supporting medium is also an important activity for the ease of the reaction in the F-T reactor. Cost evaluation is carried out to provide an assessment of the different cost items and the economic feasibility of the process.

The data and results obtained from each step will be analyzed and impact be discussed based on the case from case simulation results, coupled with comparing information with data reported in literature.

3.2 Methodology on Formulation for MEN & HEN Retrofitting

3.2.1 Process Integration

A novel and systematic technique to approach the process design problems is to use process integration including process synthesis and process analysis (El-Halwagi, 2006). This method focuses on the holistic process network as a unity, in terms of the inputs and outlets concerning the process framework. As the objective to reach the desired target through the process performance, it leads the fundamental way for insights and decisions to be placed.

Process synthesis (El-Halwagi, 2006) deals with configuration of interactive and connected process comprising of individual process elements. Therefore the structure generation and system optimization involves separating or incorporating sequential streams, calculating and analyzing the operation variables, comparing between agents and chemicals, selecting units (reactors, flashes, heat exchangers, etc.) to attain certain requirements. In order to meet the specific output target, the system needs to be revised through process synthesis, with the process inputs and outputs chosen, while the process flowsheet structure and component to be determined. The process synthesis illustration is described in Fig. 3.3.

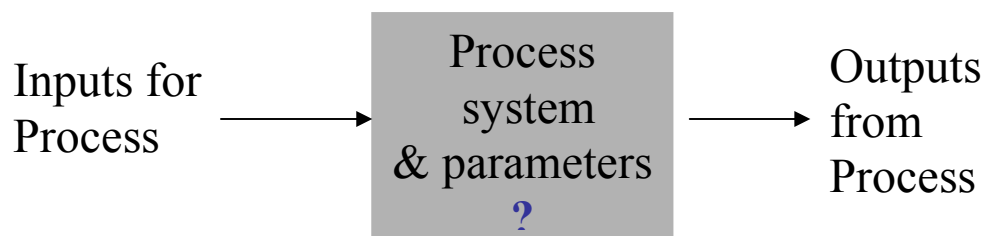


Figure 3.3. Process synthesis problems

In contrast to process synthesis (El-Halwagi, 2006), process analysis divides the whole process into its constituent components, behaving as a complement for combining individual process elements into a holistic whole for individual performance assessment. Hence, the process detailed characteristics (e.g., temperature, flow rates, compositions, and heat duty) are studied through analysis technologies as soon as the process is synthesized or an alternative is revised. These techniques involve mathematical models, empirical prediction functions, and computer-aided process simulation tools. Furthermore, predicting pilot performance and confirming experimental data also touch the border of process analysis, however the scale is. In existing facilities this is usually a common resort to validate the operation and investigation going on through the process. The process analysis statement is put here in Fig. 3.4.

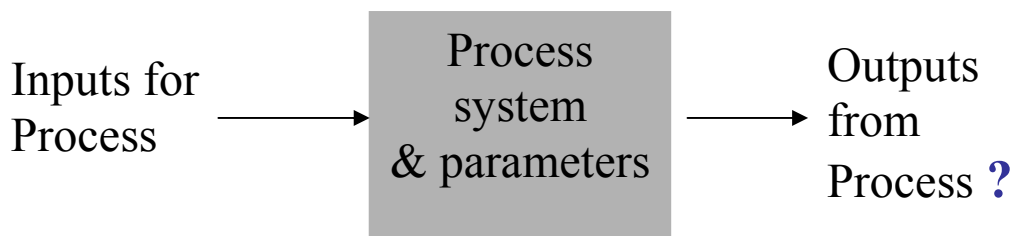


Figure 3.4. Process analysis problems

Traditional approaches to the improvement of the process solving is limited by some inevitable shortcomings, blocking the way to either real case modeling or feasible operation, which are listed as below (El-Halwagi, 2006)

- Oversimplified models that will erect inaccurate results supposed to cover general cases while in reality not (e.g., fixed value of heat transfer coefficient, pre-determined heat-exchanger types, etc.)
- Adopted solutions that are evolved from earlier scenarios, not reliable for different plants

- Complicated mathematical formulations that may not be globally solvable, resulting in only local optimum schemes or requiring more burdened work capacity

This objective is to step on a novel procedure that enjoys the following features:

- Systematically finds matches between the integrated mass streams and heat exchangers
- Identifies complicated output and input for actual case
- Allows rigorous simulation

The activities involving process integration is framed out and conducted as follows in an effective mode (El-Halwagi, 2006)

- Task identification

Task identification is the advent of the process integration step. This step locks the specified goal and the tasks based on the consideration of the input to the process. While expressing the production and output, quality and economy should also be managed.

- Targeting

Targeting is the most amazing part of the process, as it comes up with how far the bound can go, what specific potential the parameter can reach, without resorting to the detailed procedures and technologies. So emphasized again, it falls on the holistic system instead of the individual one. In this regard, this is a convenient way to specify and effective way to implement.

- Generation of alternatives (synthesis)

It is necessary to reach all configurations of interest for the process since there is a mountain of alternative choices. Once the design space is broadened, it's effective to represent alternatives and solutions to obtain the defined aim.

- Selection of alternatives (synthesis)

It is instructive to identify the optimum solutions from among the possible options, after the system with the suitable generated elements embeds the appropriate alternatives. The

selection of the optimum solutions can be verified with the help of such methods as algebraic, graphical, and mathematical optimization software.

- Analysis of selected alternatives

Process analysis techniques are brought into play to elaborate the selected alternatives. The evaluation comes to design test, hazard executive, economic assessment, environmental discussion, etc.

Process integration can be generally classified into two categories in the standing of mass and energy perspectives. One is mass integration and the other energy integration. Mass integration stands on mass and species to investigate the combination, separation, and coping of different streams to facilitate the overall performance of the resources from the streams with the assistance of the flexibility of the structure. In the same mean, energy integration generates, allocates, and exchanges energy (heat, power & work) in between process units to enhance the quality and consumption of the process, which will be talked about in later parts.

3.2.2 Strategies in Mass-Integration

Consider a mass exchange network, once the target is set, it's possible to segregate the streams to some fraction, feed them to certain sinks, and then mix the splits of streams to some extent to designate an optimum way, claiming minimum fresh input, minimum waste out, and maximum recycle of the raw materials. So questions come as how to deal with the recycling, how to alter the existing operation conditions. The design decisions can be constructed in Fig. 3.5.

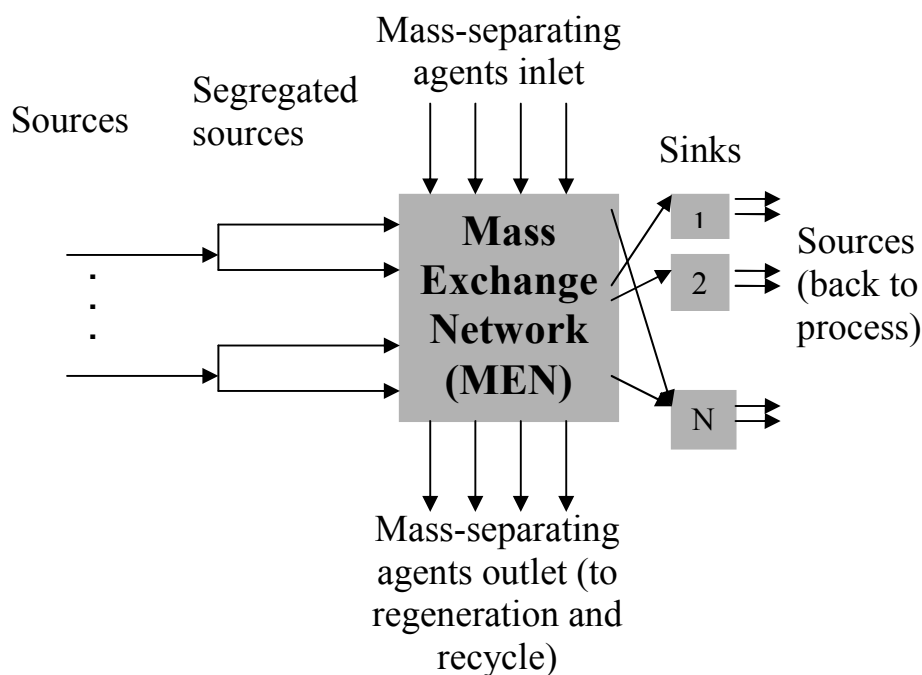


Figure 3.5. Process from species perspective when integrated (El-Halwagi, 2006)

Based on fundamental principles of chemical analysis, this provides the global identification and allocation of the performance in agents treatment. Mass balance and equilibrium functions are most enjoyed in the calculations. The system could be classified into process sinks and process sources. Process sinks are units accepting the species, thus streams leaving sinks will twist to sources supplying species. In this regard, altering the design operations influencing flowrates and concentration will in turn manipulate the sinks.

Fresh sources for the targeted species are possibly replaced by equivalent recycling streams from intermediate process outlet streams, on the condition that flowrate and composition constraints are met. After that recycle or reroute can be undertaken to attain the target. However, if the conditions don't stand, it's necessary to intercept the outlet streams until they can take the task of replacement.

Here is the graphical illustration of the source and sink interaction problem. As we already indicated, the identification of the performance is ahead of the detailed strategies. First, the sinks are ranked in order of sequential increasing admissible composition way. The same is done to rank the sources. Place each sink's maximum load of impurities versus its flowrate in the coordinate, one after one, constructing the sink composite curve, in the ascending order. The sources composite curve is developed, without considering where the starting arrow tail will be plotted. In all, it's an accumulative representation of all sinks and sources showing the upper feasible bound in the diagram region. It is worth to mention the source stream curve is then moved horizontally until it touches the sinks composite curve where overlap is forbidden. From the diagram the material recycle pinch point is designated as the point where they touch, shown in Fig. 3.6. There are some rules for the design method, allowing no flowrate to pass through the pinch point, no waste to leave from sources below the pinch point, and no fresh to feed in the sink above the pinch point (El-Halwagi, 2006). The key reflection observed from the diagram is characterized from the distinguished zones. The extent between the source curve and sink curve on the horizontal axis corresponds to minimum fresh usage, and in the same manner, the maximum recycle amount and the minimum waste discharge are identified from the diagram considering pure fresh.

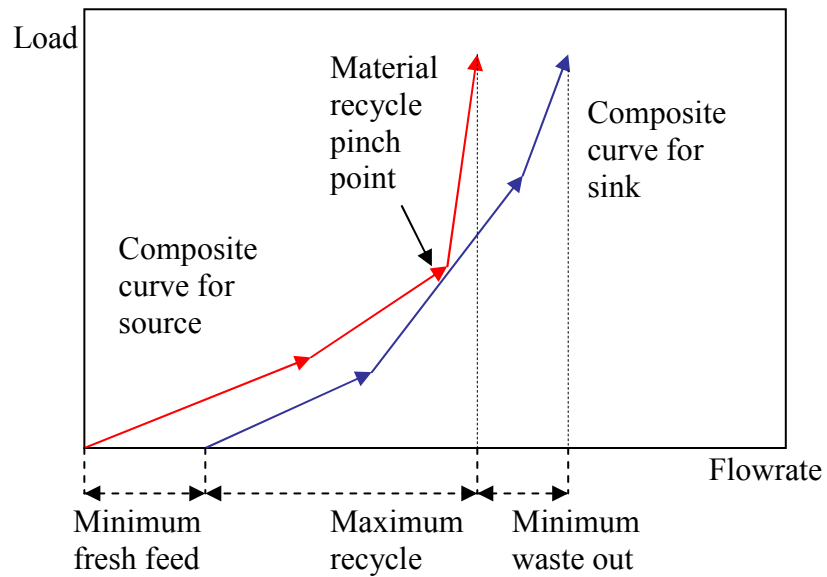


Figure 3.6. Identifying pinch point for maximum recycling (El-Halwagi, 2006)

To identify targets for direct recycle problems, algebraic approach is also beneficial to develop providing useful insights. For large amounts of sources and sinks, and scaling problems as well, a broader task should be handled. It's easy to put the problem into an interval cascade diagram to illustrate. The most negative residual in the diagram indicates the minimum fresh input for the process, with the sinks and sources calculations for each interval shown (Fig. 3.7).

This procedure constitutes the basis for the material rerouting strategy. The advantage is to facilitate the designer's effort and to ensure the process capabilities. In the spirit of integration, targeting is put over the detailed technique of each unit. To summarize it, the data and models are generated from the fundamental information, before minimizing the net generation. Next, design and variables are adjusted to minimize the fresh usage and recover the load system. Then the whole material balance is formulated regarding the feed and waste, to aim the target.

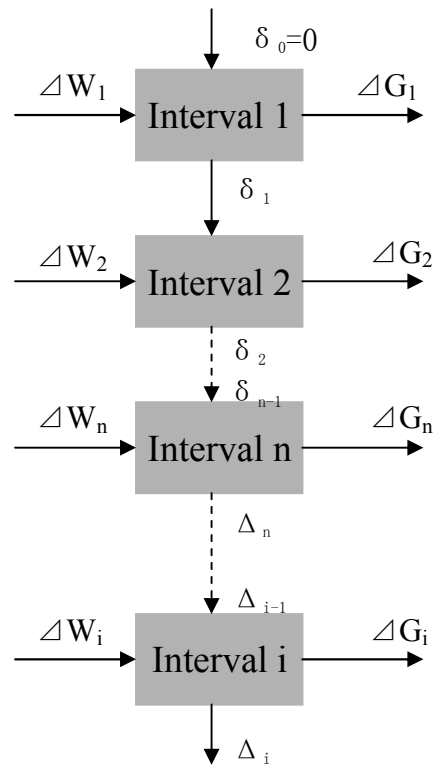


Figure 3.7. Cascade diagram for mass integration (El-Halwagi, 2006)

3.2.3 Method for HENs

In a typical process, heat is one of the most significant factor concerning heating, cooling, power generation and consumption, shedding the light on the attention to pay to the heat integration. This kicks off to the important role HEN plays. An HEN (heat exchange network) is a network taking use of existing heating utilities and framework to effectively save energy (El-Halwagi, 2006). Therefore synthesis and analysis of heat are applied to address the performance for most industrial facilities. It plays normally with hot streams and cold streams and the potential that can be extract between them. For the overall scheme, the feeds into and the flows from the unit are illustrated in Fig. 3.8. The supply and targeting temperature and heat capacity are provided to calculate the required external utilities.

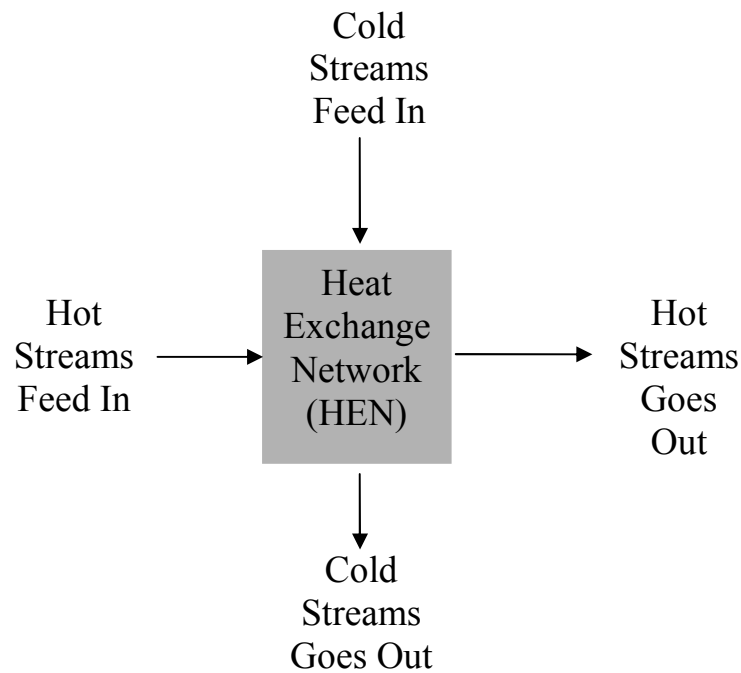


Figure 3.8. Heat exchange network (HEN) synthesis (El-Halwagi, 2006)

One of the major methods (El-Halwagi, 2006) is thermal pinch analysis, drawing support from graphical technique. In this context, after the heat exchange from the process streams are maximized, the minimum usage of utilities can be obtained.

Consider a process with a number N_H of hot streams and a number N_C of cold streams, the heat are exchanged by each stream. For the u th hot stream, the heat exchanged by it can be set as (El-Halwagi, 2006)

$$HH_u = F_u C_{p,u} (T_u^s - T_u^t) \quad (3.1)$$

where

T_u^s is supply temperature for uth hot stream

T_u^t is target temperature for uth hot stream

$F_u C_{p,u}$ is heat capacity for u th process hot stream

HH_u is heat exchange from the u th hot stream

$u=1, 2, \dots, N_H$

At the same time, the heat exchanged by the v th cold stream is set as

$$HC_v = f_v C_{p,v} (t_v^s - t_v^t) \quad (3.2)$$

where

t_v^s is supply temperature for v th cold stream

t_v^t is target temperature for v th cold stream

$f_v C_{p,v}$ is heat capacity for v th process cold stream

HC_v is heat exchange by the v th cold stream

$v=1, 2, \dots, N_C$

Each stream can be arranged by heat capacity ascending order with head and tail connecting on the plot of enthalpy exchange versus temperature function (El-Halwagi, 2006). The temperature for the hot stream is plotted in T , while that for the cold stream is plotted in cold scale t , where $T = t + \Delta T^{\min}$ is assumed to satisfy the second law of thermodynamics. Different heat exchange can be decided by moving cold composite stream curve vertically in the diagram. When the cold composite curve touches the hot stream curve, it means the optimum target arrives leaving no space or overlap between the two curves in horizontal level. As a result, the thermal pinch point is gained at the point shared by the cold and hot composite stream curves. We can find the minimum heating and cooling utilities from the Fig. 3.9. It also shows the maximum integrated heat exchange that can be targeted without detailing the complicated measures taken to fulfill the task.

Another way for the targeting of the integrated heat exchange is algebraic method, providing quantitative data. It complements graphical method with more insights into the specific transfer heat exchanged between each level of temperature unit. It includes three

steps: temperature-interval diagram (TID), table of exchangeable heat loads (TEHL) and the cascade diagram.

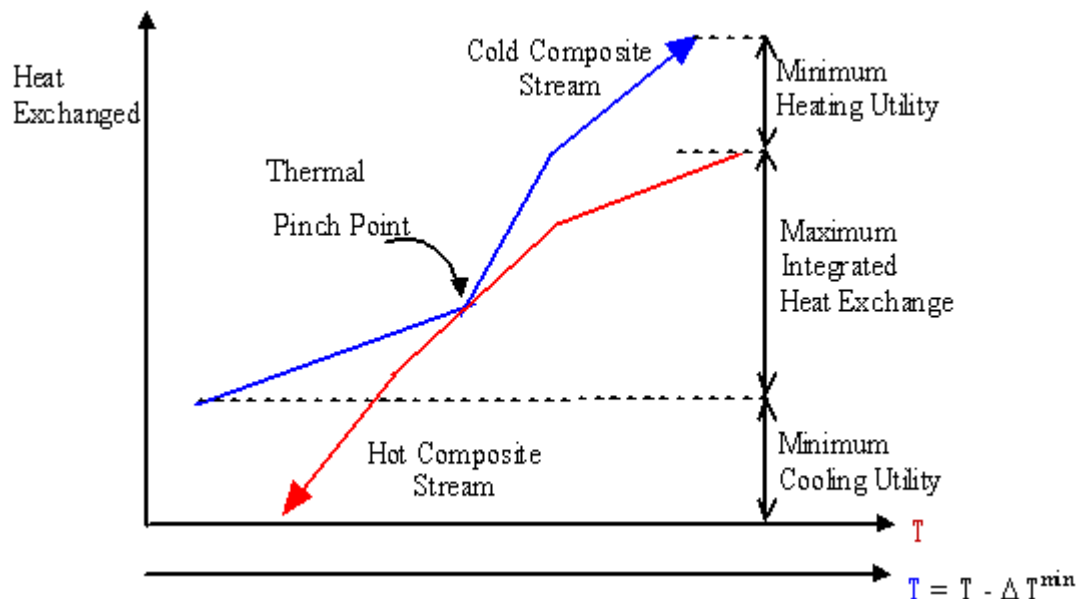


Figure 3.9. Thermal pinch diagram (El-Halwagi, 2006)

In TID, numerous temperature intervals are defined with each line indicating each required temperature. The arrows show the target and supply temperature for each stream in the process. Since it is thermodynamically possible and feasible to transfer heat from the hot stream to the cold stream in the same interval (El-Halwagi, 2006) and from an interval to any one below it by hot streams, the heat exchange network is solved with this manner. Fig. 3.10 gives a brief example of temperature-interval diagram (TID).

This bases the way for the next step, a table of exchangeable heat loads (TEHL). This comprises of series of temperature intervals mentioned above. For each interval, the exchangeable heat is calculated (El-Halwagi, 2006).

The exchangeable heat by the v th hot stream going through the z th interval is expressed as (El-Halwagi, 2006)

$$HH_{u,z} = F_u C_{p,u} (T_{z-1} - T_z) \tag{3.3}$$

where

T_{z-1} , T_z are the bottom and top temperature for the z th interval from the hot stream.

The exchangeable heat by the v th cold stream going through the z th interval is expressed as

$$HC_{v,z} = f_v C_{p,v} (t_{z-1} - t_z) \tag{3.4}$$

where

t_{z-1} , t_z are the bottom and top temperature for the z th interval to the cold stream.

Interval	Hot Stream	Cold Stream
	T_{H1}^{in}	$T_{H1}^{in} - \Delta T^{min}$
1	$T_{C1}^{in} + \Delta T^{min}$	T_{C1}^{out}
2	$T_{C2}^{out} + \Delta T^{min}$	T_{C2}^{out}
3	T_{H2}^{in}	$T_{H2}^{in} - \Delta T^{min}$
4	T_{H1}^{out}	T_{C1}^{in}
5	$T_{C2}^{out} + \Delta T^{min}$	T_{C2}^{out}
6	T_{H3}^{int}	$T_{H3}^{in} - \Delta T_{min}$
7	$T_{C2}^{in} + \Delta T^{min}$	T_{C2}^{in}
8	T_{H2}^{out}	T_{C3}^{out}
9	$T_{C3}^{in} + \Delta T^{min}$	T_{C3}^{in}
10	T_{H3}^{out}	$T_{H3}^{out} - \Delta T_{min}$

		T_{CN}^{in}
N	T_{HN}^{out}	

Figure 3.10. Temperature-interval diagram (El-Halwagi, 2006)

Fig. 3.11 shows the heat balance around the z th interval.

To get the total load of capacity around the z th interval it is necessary to sum up the heat capacity of each stream that passes through that interval

$$HH_z^{Total} = \sum_{\substack{u \text{ passes through interval } z \\ \text{where } u=1,2,\dots,N_H}} HH_{u,z} \quad (3.5)$$

$$HC_z^{Total} = \sum_{\substack{v \text{ passes through interval } z \\ \text{and } v=1,2,\dots,N_C}} HC_{v,z} \quad (3.6)$$

The heat balance can be expressed by the following equation for each temperature interval, in order to get the overall heat needed to transfer within the process to check where the thermal pinch point is.

$$r_z = HH_Z^{Total} + HHU_z^{Total} - HC_Z^{Total} - HCU_z^{Total} + r_{z-1} \quad (3.7)$$

where

r_{z-1}, r_z are the residual heats to and from the z th interval (El-Halwagi, 2006)

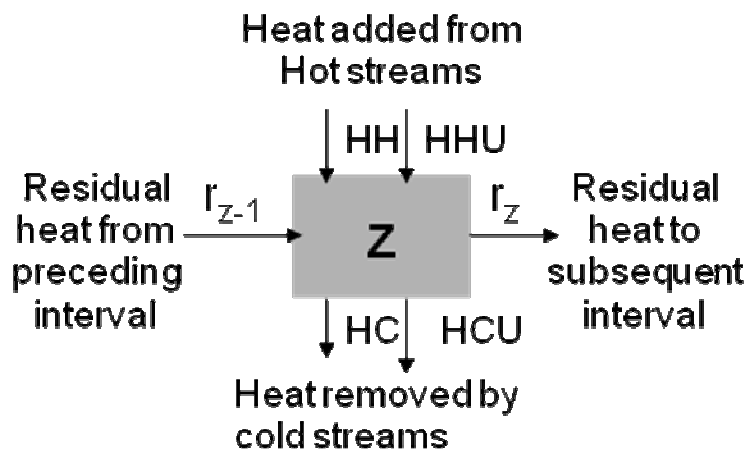


Figure 3.11. Heat balance around a temperature interval (El-Halwagi, 2006)

A negative r_z tells that the residual heat is passing up which is thermodynamically infeasible. To bring the diagram to a feasible way, a hot capacity equivalent to the most negative residual heat is added, which is also the minimum heating utility required corresponding to the result from graphical heat integration method. And minimum cooling utility corresponds to the residual from the bottom interval, with the zero residual point matching the thermal pinch point. The detailed information for each interval is shown from Fig. 3.12.

3.2.4 Combined Heat and Power Integration

When work is introduced, energy integration can be more complete with the perspective of both generation for heat and work. Usually it takes an engine to the pinch diagram, either discharging or interacting the heat. For HEN (El-Halwagi, 2006), the places above the pinch point heat is strongly needed, so high temperature heat source engine could be placed to provide the minimum heat, generating work simultaneously. While for the region below the pinch point, heat is in surplus form, indicating they can be discharged to low temperature heat sink engine, generating work at the same time. This idea can be represented in the Fig. 3.13 (El-Halwagi, 2006). So this leads to the task to identify the cogeneration target for the process. For example, steam can be used serving both the power producing function and the process stream. If releasing high pressure steam to lower pressure, power can be produced, and this extractable energy can be coupled with the turbine action.

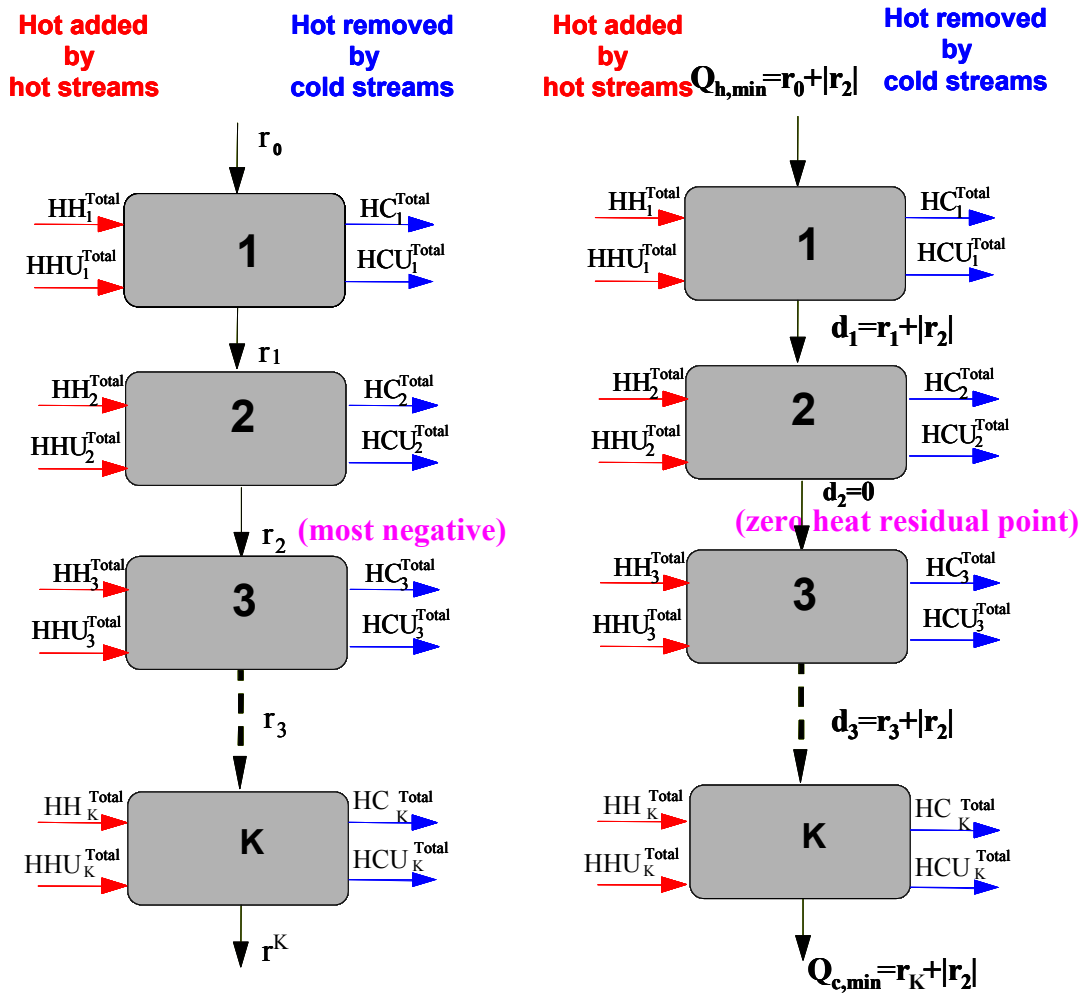


Figure 3.12. Cascade diagram for HENs (El-Halwagi, 2006)

Based on all the measures, procedures are proposed to acquire the heat target, which are listed in Fig. 3.14.

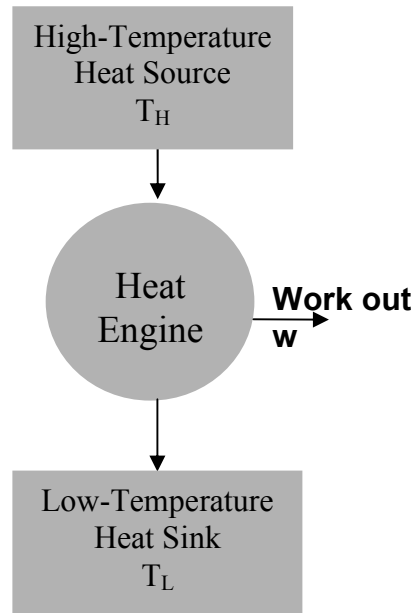


Figure 3.13. Placing of the heat engine for the HEN

In order to determine the target for process cogeneration, the procedure of (El-Halwagi, 2006) will be used. First, we start by considering the combustible wastes in the process that will provide surplus steam. The demand headers represent the process needs of steam. For an isentropic turbine operating between two headers, the enthalpy change can be determined as:

$$\Delta H^{isentropic} = H^{in} - H_{is}^{out} \quad (3.8)$$

where $\Delta H^{isentropic}$ is the specific isentropic enthalpy change in the turbine, H^{in} is the specific enthalpy of the steam at the inlet temperature and pressure of the turbine and H_{is}^{out} is the specific isentropic enthalpy at the outlet pressure of the turbine. The isentropic efficiency term is defined as follows:

$$\eta_{is} = \frac{\Delta H^{real}}{\Delta H^{isentropic}} \quad (3.9)$$

where η_{is} is the isentropic efficiency and ΔH^{real} is the actual specific enthalpy difference across the turbine. For a given flowrate of steam passing through the turbine, \dot{m} , the power produced by the turbine, W , is given by:

$$W = \dot{m} \eta_{is} (H^{in} - H_{is}^{out}) \quad (3.10)$$

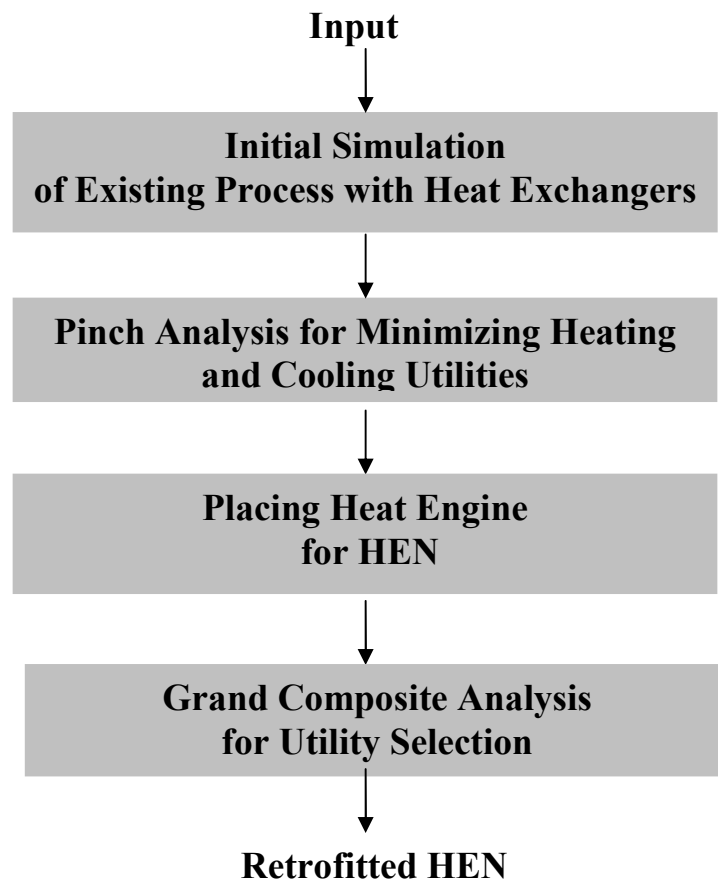


Figure 3.14. Overview of the strategies for the application

In order to avoid performing detailed turbine calculations at the level of targeting, El-Halwagi (El-Halwagi, 2006) introduced the term “*extractable energy*” which is based on the actual conditions of the headers.

$$e_{Header} = \eta_{Header} H_{Header} \quad (3.11)$$

where e_{Header} is the extractable energy for a given header, η_{Header} is an efficiency term and H_{Header} is the specific enthalpy at a given set of conditions for the header. The extractable power, E_{Header} , of a header is defined as:

$$E_{Header} = \dot{m} \eta_{Header} H_{Header} = \dot{m} e_{Header} \quad (3.12)$$

The power generation expression can be rewritten as the difference between the inlet and outlet extractable power:

$$W = E^{in} - E^{out} \quad (3.13)$$

where E^{in} is the extractable power at the header conditions feeding the inlet steam to the turbine and E^{out} is the extractable power at the header conditions receiving the outlet steam from the turbine. By developing composite representations of the surplus and deficit steam headers and using the concepts of extractable power, a cogeneration targeting pinch diagram is developed to determine to cogeneration potential and excess steam as show in Fig. 3.15.

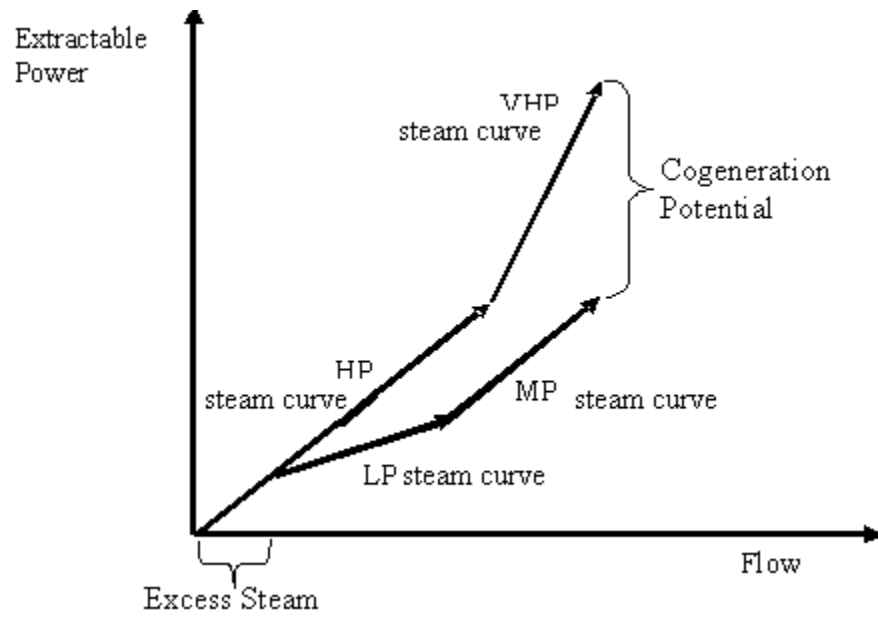


Figure 3.15. Extractable power cogeneration targeting pinch diagram (El-Halwagi, 2006)

4 CASE STUDY

4.1 GTL Process Description

Consider a base-case GTL process which uses natural gas as a feedstock. The process involves three steps: reforming, F-T reaction, and upgrading. First, natural gas is preheated and sent into an autothermal reactor to react with steam and oxygen. The temperature of the syngas from the reactor is too high to be fed into the F-T reactor. Therefore, the syngas stream is cooled down and water is separated out. The syncrude from the F-T reactor is fed to distillation columns to produce different hydrocarbon fractions which are referred to as GTL products, and the tailgas is introduced through cooling equipment and water separation equipment to final treatment or to recycle. Fig. 4.1 is a schematic representation of the base-case flowsheet.

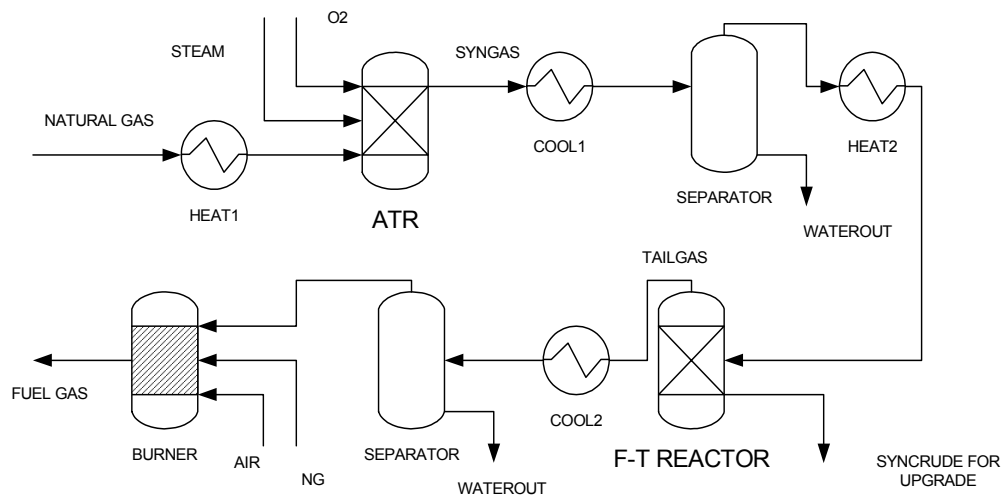


Figure 4.1. Schematic representation of the base-case GTL flowsheet

The design specifications and requirements are discussed in the following sections on the basis of feed, product, and operating conditions of the units.

4.2 Design Basis and Specifications

4.2.1 Feed Conditions

The case study deals with a feedstock of natural gas. Table 4.1 lists the characteristics of the natural gas fed to the process.

Table 4.1. The feed gas conditions (Al-Sobhi, 2007)

Flowrate (kg/hr)	30,000
Temperature (°C)	26
Pressure (bar)	26
Component	Composition (mol%)
methane	95.39
ethane	3.91
propane	0.03
CO ₂	0.59
N ₂	0.08

4.2.2 Process Specifications

For the stream fed to the autothermal reactor, the mole fraction of water to methane is set to be 1.3. Additionally, the molar ratio of oxygen to methane is specified to be 0.6 in the feed to the autothermal reactor. Because of the numerous compounds existing in the F-T product stream, few model compounds are selected to represent the stream while providing a proper description of the ASF distribution. Table 4.2 gives the list of representative compounds produced from the F-T reactor modeling the type of slurry phase reactor.

Table 4.2. Composition of the products from the F-T reactor

Component	Mass%
CH ₄	0.91
N ₂	11.57
C ₂ H ₆	0.13
C ₃ H ₈	10.13
C ₂₆ H ₅₄	27.64
C ₁₉ H ₄₀	30.59
C ₉ H ₂₀	11.09
C ₉ H ₁₈	7.94
C ₉ H ₁₈ O ₂	0.90
Total	100.00

4.2.3 Conditions for the Main Units

The thermodynamic properties of the streams were modeled using NRTL-RK property method. The autothermal reactor is simulated with the ASPEN Plus REquil model which is an equilibrium-based calculation. The pressure and temperature of the autothermal reactor are set at 18 bar and 1300 K, respectively. The syngas usage ratio (H₂/CO) produced from this unit is better to keep around 2 as mentioned in the introduction before. The extent of reactions in the F-T reactor is adjusted so as to meet the desired ASF distribution; the distribution of products for this case is illustrated in Fig. 4.2. The pressure is maintained at 30 bar and temperature is set to be 510 K. To properly model the upgrading system, it is important to have a feed that represents the distillation curve (or boiling point fraction assay) of the syncrude produced from the F-T reactor, and the boiling curve for this case is shown in Fig. 4.3.

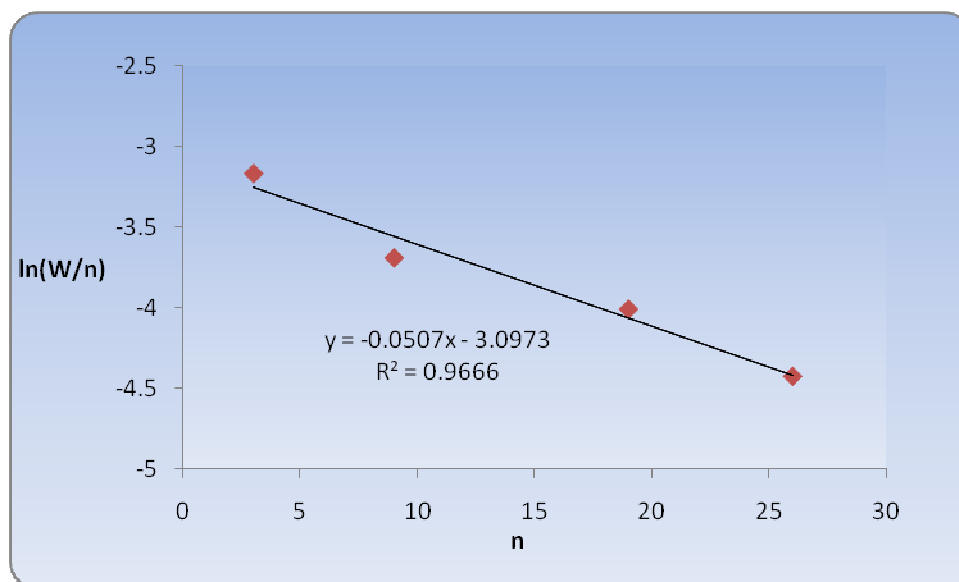


Figure 4.2. Products distribution following ASF

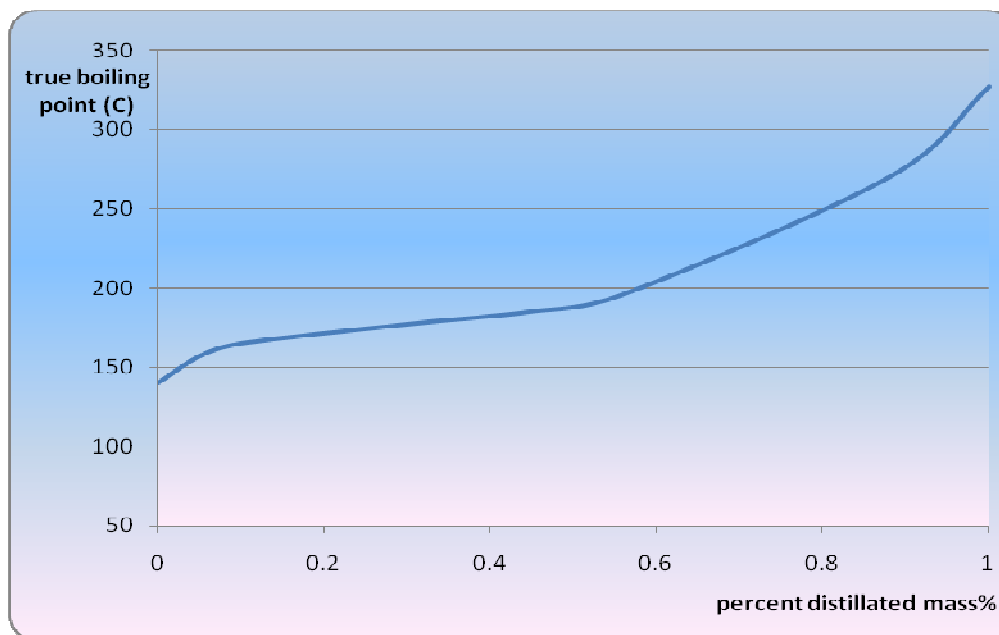


Figure 4.3. Products boiling point curve

4.2.4 Utilities

The cooling and heating utilities conditions and costs are listed in Table 4.3.

Table 4.3. Conditions and costs of the heating and cooling utilities

Utility Name	Type	Temperature (° F)		Pressure (psia)	Cost
		in	out		
Low pressure steam	Cooling	75	95	50	\$4.0 / MMBtu
High pressure steam	Heating	510	501	350	\$6.8 / MMBtu
High temperature heating oil	Heating	1055	1015	25	\$23 / MMBtu
Water	Cooling	80	90	1.0	\$0.4 / ton

Other operating utility prices include: Electricity is 0.064 \$/ kWh and Gas is 8.3 \$/ MMBtu.

resulting ratio of H_2/CO in the syngas changes from 1.8 to 3.2. When the molar ratio of oxygen to methane is about 0.5, the syngas usage ratio is close to 2.0. When this ratio goes beyond 0.6, there is little change in the value of the syngas usage ratio (still around 2.0). This suggests that there is not much benefit for increasing the O_2/CH_4 ratio beyond 0.6. The same approach is used for the selection of the H_2O/CH_4 ratio, and it comes out that a molar ratio of 1.3 works well.

For the upgrading step, the products produced are in vapor and liquid forms. The vapor fraction is separated out as tailgas to be either recycled or burned. The liquid fraction comprises the majority of the syncrude which is mostly hydrocarbon with little water. The syncrude is fed into a distillation column to separate the different boiling fractions with the major parts being LPG, naphtha and wax. Table 5.1 gives a description of the carbon range for the different cuts. The simulation results for the compositions of the distillation products are shown in Table 5.2.

Table 5.1. Syncrude fractions (Zhang, 2000)

LPG	C_2-C_4
gasoline	C_5-C_{12}
Diesel oil	$C_{13}-C_{18}$
wax	C_{19+}

Table 5.2. Compositions (mass%) of the streams leaving the distillation columns

STREAM FRACTION	HEAVY DIESEL	LIGHT DIESEL	TOP	WAX
LPG	3.37E-15	5.08E-01	4.23E+01	1.99E-29
NAPHTHA	7.67E-06	1.46E+01	5.73E+01	2.34E-14
LIGHT DIESEL	3.84E+00	8.48E+01	3.81E-01	1.21E-05
HEAVY DIESEL	7.37E+01	1.07E-01	8.80E-11	2.94E+01
WAX	2.24E+01	7.27E-12	5.31E-35	7.06E+01

5.2 Process Mass and Heat Balance

The mass balance for the whole GTL process is listed in Tables 5.3.

Table 5.3. Mass balance for GTL process

Components (kg/hr)	Feed in		Syncrude	Water out	Tail gas out
Water	1,195,020	=	0	1,143,720	586,320
Natural gas	896,280		0	0	0
O₂	990,000		0	0	0
CO	0		0	0	122,580
H₂	0		0	0	73,950
CO₂	0		0	0	604,500
>C₄	0		476,430	0	0
OTHER	0		0	0	73,830
Total mass	3,081,300		476,430	1,143,720	1,461,180
Total volume	1,158,171,540 SCF/D		224,640 GAL/hr 128,000 BPD		

The heat balance around each unit is listed in Table 5.4. It shows that the F-T reactor produces the majority of heat which may be used for power cogeneration. Furthermore, when the tail gas is burned, it can provide additional heat. As such, special attention should be given to power cogeneration in this GTL process.

Table 5.4. Heat duty for each unit in the GTL process (positive numbers indicate heat to be added while negative numbers represent heat to be removed)

Units	Enthalpy (Btu/hr)
Heat 1	2.9E+09
Heat 2	1.2E+09
Cool 1	-9.9E+09
Cool 2	-6.5E+08

5.3 Heat Integration and Targeting

The description of hot and cold streams is illustrated in Fig. 5.2.

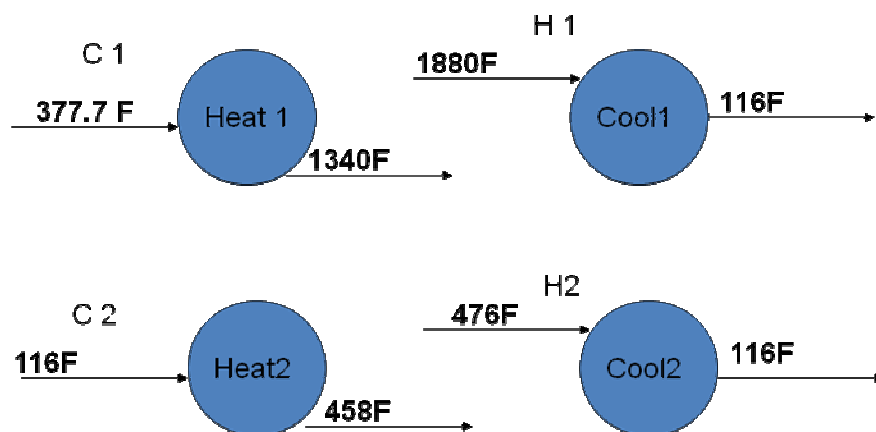


Figure 5.2. Description of the hot and cold streams

Then thermal pinch analysis is conducted to determine the potential heat that could be exchanged among the hot and cold streams. The savings for heating and cooling utilities resulting from heat integration are listed in Table 5.5. As described before, the construction of the temperature interval diagram is followed in Fig. 5.3. A minimum approach temperature of 10 K is assumed. Next, the table of exchangeable heat loads (TEHL) for the process hot and cold streams is conducted in Tables 5.6 and 5.7. Later, the cascade diagram is constructed to check the thermal pinch point, shown in Fig. 5.4.

The grand composite curve is shown in Fig. 5.5. The most negative value from the cascade diagram shows the thermal pinch point, and by adding external heating utility from the top the minimum utility requirement will be got. However, from this diagram it indicates that the configuration is already in the optimum and the heat flows downward. So the minimum cooling utility is 6.16 billion Btu/hr and heating utility is 0.

Table 5.5. Heating and cooling utilities savings

	Heating utilities (Btu/hr)	Cooling utilities (Btu/hr)
before integration	4.2E+09	10.6E+09
after integration	0	6.16E+09
Savings (\$/yr)	100% 671,071,380	41.8% 213,378,132

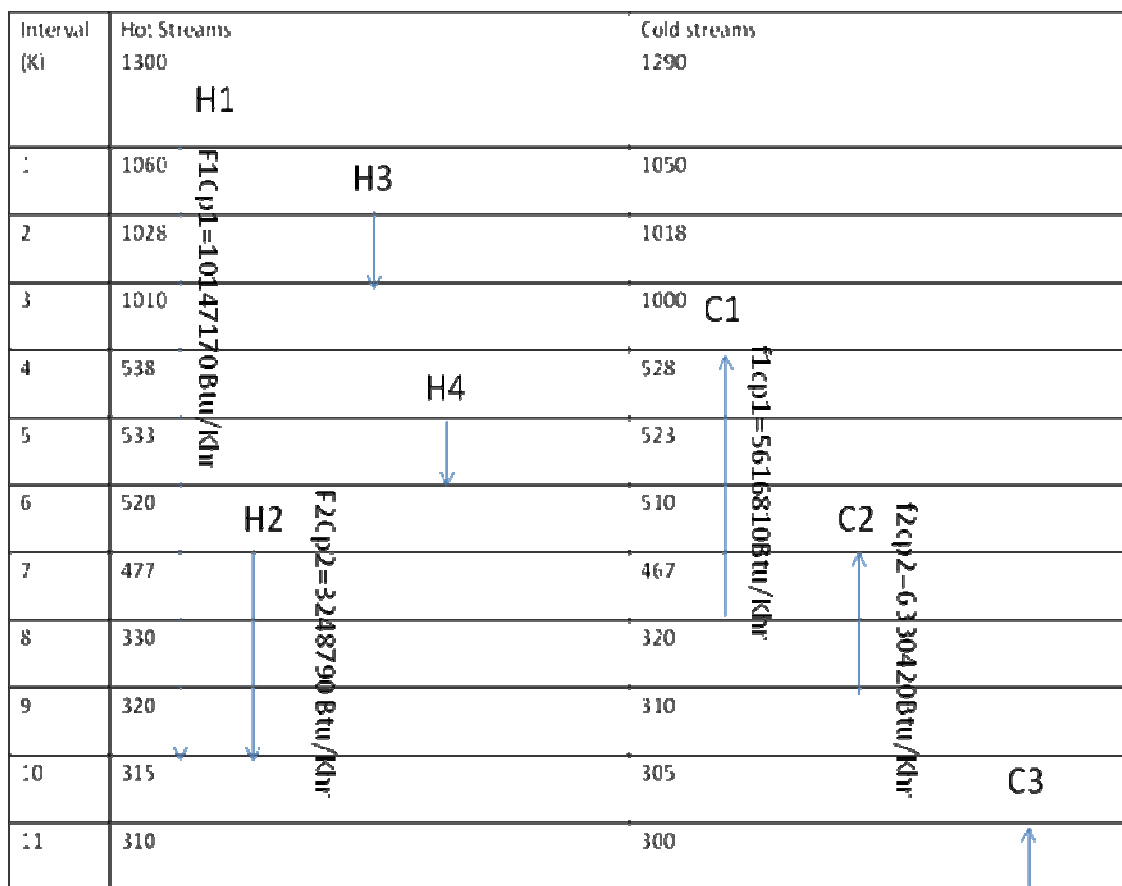


Figure 5.3. Temperature interval diagram for the GTL process

Table 5.6. TEHL for process hot streams

Interval	Capacity of H1 (Btu/hr)	Capacity of H2 (Btu/hr)	Total capacity (Btu/hr)
1	2,435,320,800	0	2,435,320,800
2	324,709,440	0	324,709,440
3	182,649,060	0	182,649,060
4	4,789,464,240	0	4,789,464,240
5	50,735,850	0	50,735,850
6	131,913,210	0	131,913,210

Table 5.6. Continued

7	436,328,310	139,697,970	576,026,280
8	1,491,633,990	477,572,130	1,969,206,120
9	101,471,700	32,487,900	133,959,600
10	0	0	0
11	0	0	0

Table 5.7. TEHL for process cold streams

Interval	Capacity of C1 (Btu/hr)	Capacity of C2 (Btu/hr)	Total capacity (Btu/hr)
1	0	0	0
2	0	0	0
3	0	0	0
4	2,651,134,320	0	2,651,134,320
5	73,018,530	0	73,018,530
6	241,522,830	0	241,522,830
7	241,522,830	272,208,060	513,730,890
8	0	930,571,740	930,571,740
9	0	0	0
10	0	0	0
11	0	0	0

5.4 Heat Engine and Cogeneration Targeting

From the cascade diagram discussed in previous section, it is possible to place a heat engine at the bottom of the cascade to discharge heat to a low temperature heat sink which can be coupled to an LNG process refrigerant step, for example, to 250 K. In such cases, the Carnot efficiency may be calculated as:

$$\eta = 1 - \frac{T_C}{T_H} = 1 - \frac{250}{305} = 0.18 \quad (5.1)$$

Assuming Q_{out} is 3,000,000,000 Btu/hr, thus the power may be calculated by:

$$W = \eta * Q_{out} / (1 - \eta) = 658,536,570 \text{ Btu/hr} \quad (5.2)$$

$$\text{and the inlet heat: } Q_{in} = Q_{out} / (1 - \eta) = 3,658,536,570 \text{ Btu/hr.} \quad (5.3)$$

With this integration the cooling utility is reduced from 6,161,723,610 Btu/hr to 2,503,187,010 Btu/hr (Fig. 5.6).

Consider a couple of steam headers, high pressure (HP) and low pressure (LP). From Fig. 5.7, it can be seen that at 700 K a 350 psia HP can be generated, and by letting it down in a turbine the 50 psia LP with 450 K is obtained, and at the same time the power is generated which can significantly reduce the cost for the LP steam and power consumption. The steam information is provided in Table 5.8. The power efficiency is taken as 0.72. By plotting the extractable power versus the flow rate, the cogeneration potential is obtained in Fig. 5.7.

Table 5.8. Steam header information

Header	Pressure (psia)	Specific enthalpy (Btu/lb)	Flow rate (lb/hr)	Net enthalpy difference per hour (Btu/hr)	Extractable power (Btu/hr)
HP	350	1,205	3,734,000	4.5E+09	3.2E+09
LP	50	1,174	4,344,000	5.1E+09	3.6E+09

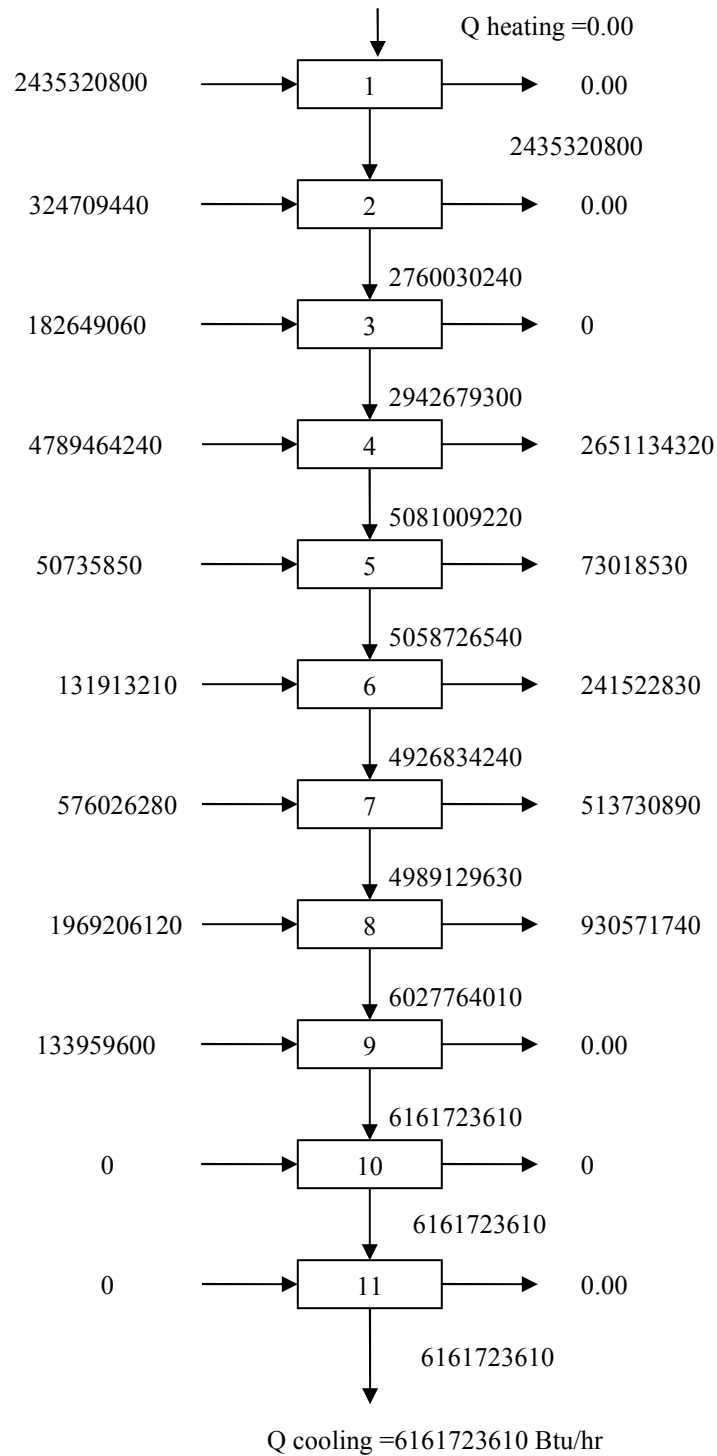


Figure 5.4. Cascade diagram for the GTL process

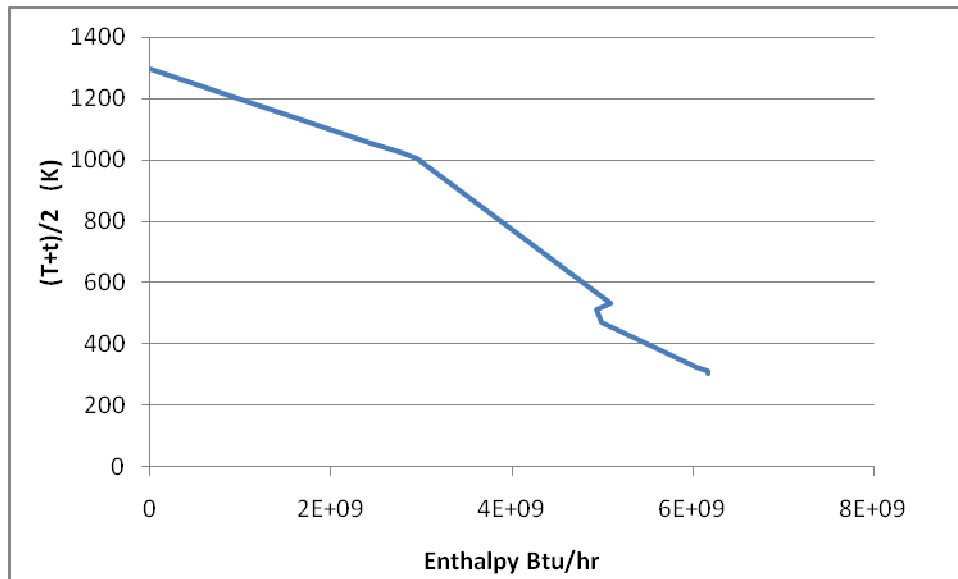


Figure 5.5. Grand composite curve for the GTL process

A steady state ASPEN Plus simulation is conducted for this case and result shows 224,000 hp (167,000 KW) power is generated from the turbine, shown in Fig. 5.8.

The value of produced power is calculated to be

$$167,000 \text{ kW} * 0.064 \$/\text{kWh} * 8760 \text{ h/yr} = 93,627,000 \text{ \$/yr} \quad (5.4)$$

And the low-pressure steam saved from this cogeneration has a value of 153 MM \$/yr

This means about 246 MM \$/yr can be saved from this cogeneration conduction.

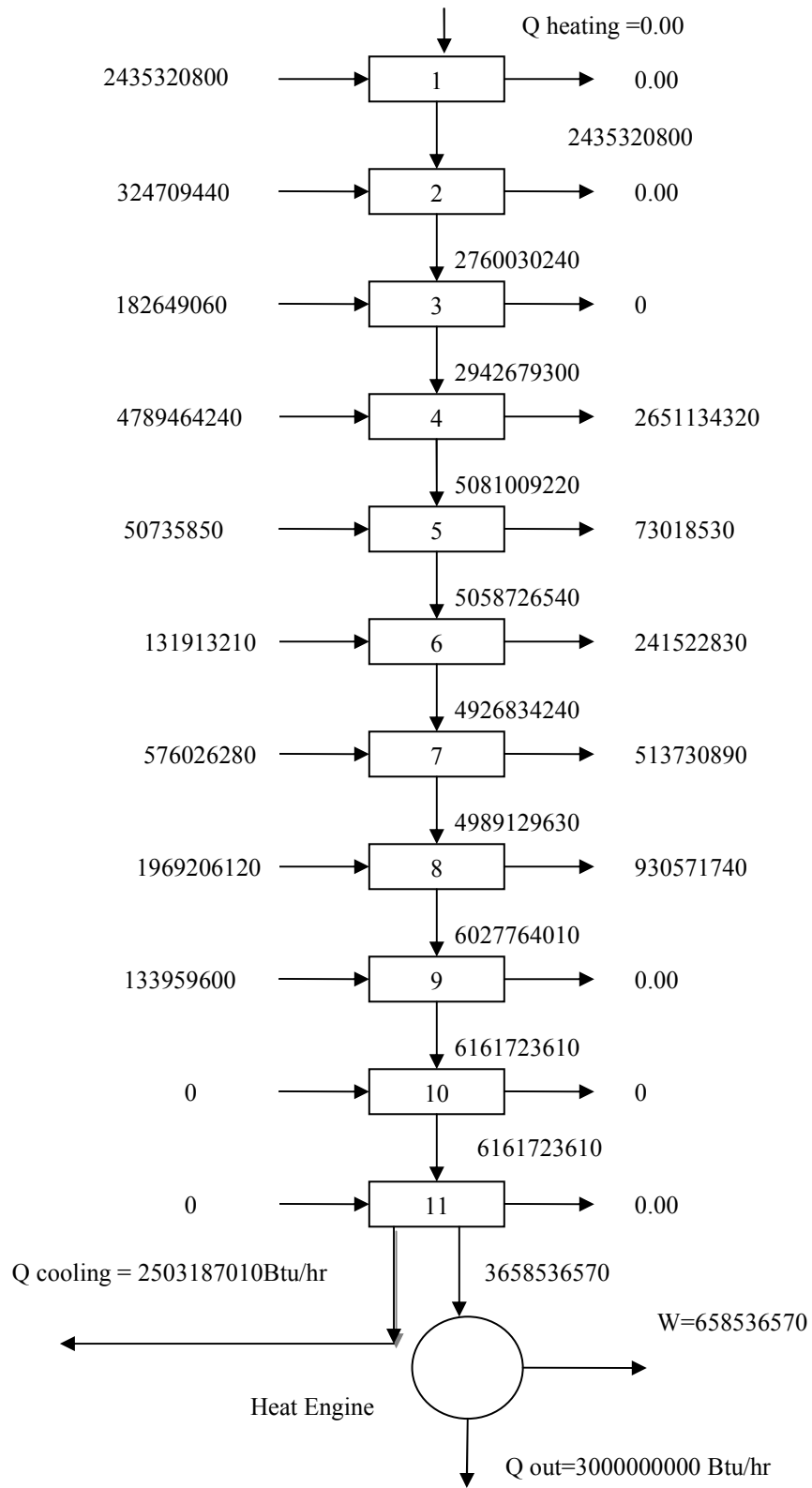


Figure 5.6. Integrating of the heat engine with HEN

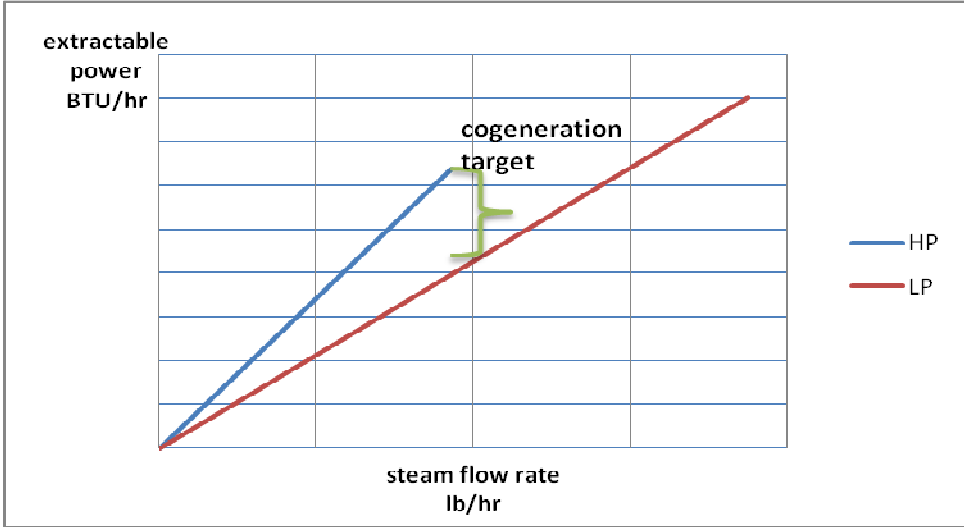


Figure 5.7. Unshifted extractable power versus flowrate plot

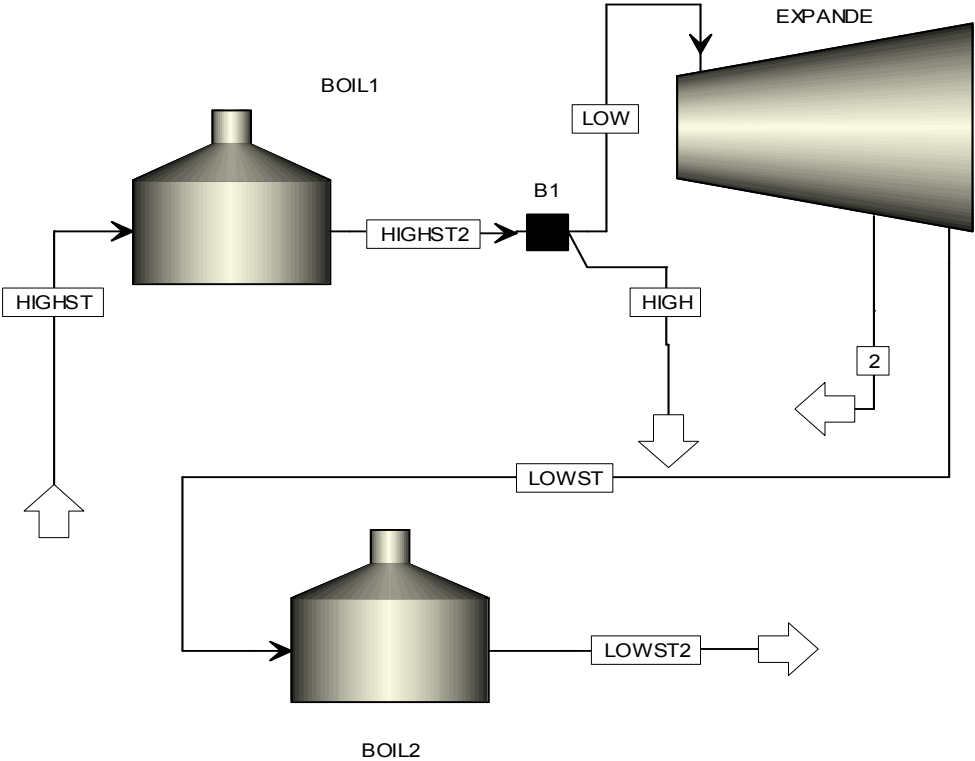


Figure 5.8. Representation of the cogeneration flowsheet

5.5 Mass Integration

There are several opportunities for mass integration. Here, focus is given to three problems:

- a. Utilization of the tail gas
- b. Recovery of catalyst-supporting medium
- c. Water management
- d. CO₂ separation

5.5.1 Utilization of Tail Gas

Based on the design and features of the GTL process, the tail gas problem is represented via a source sink mapping diagram (Fig. 5.9). The source is split into fractions that are allocated to each sink. The objective is to minimize the waste (assigned to burner), based on the mass balance calculation and species equilibrium.

Minimize burner flowrate

Subject to:

$$\text{Source} = \text{F-T} + \text{ATR} + \text{burner} \quad (5.5)$$

$$\text{Source} * \text{Source fraction} = \text{F-T} * \text{F-T fraction} + \text{ATR} * \text{ATR fraction} + \text{burner} * \text{burner fraction} \quad (5.6)$$

as well as the following constraints:

The syngas usage ratio should be kept around 2. Therefore, the maximum inlet mass fraction for F-T should not exceed 0.87. Dropping the value to lower mass fractions will negatively influence the reaction yield. If the recycle ratio is 1 to the ATR, the fractions of components will influence the reaction and thus the syngas ratio. Based on simulation analysis, the maximum flow that could be recycled to ATR is 0.25 of the tailgas flow rate. So the flow rate and fractions for each sink and source are listed in Tables 5.9 and 5.10.

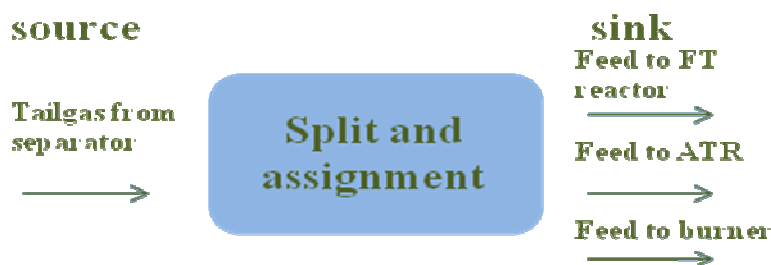


Figure 5.9. Assignment of split fractions and assignment to sinks for GTL process

Table 5.9. Source data for the GTL process

source	Flow rate (kg/hr)	Inlet mass fraction
Separator	886,470	0.138

Table 5.10. Sink data for GTL process

Sink	Flow rate (kg/hr)	Minimum inlet mass fraction	Maximum inlet mass fraction
F-T reactor	1,937,610	0.4	0.875
ATR	2,091,360	0	1
Burner	?	?	?

From the abovementioned discussions, the mass integration suggests 0.25 ratio of recycle for the tailgas to the ATR, intending to reserve resources and also keep a high yield for the syncrude produced.

5.5.2 Recovery of the Catalyst Supporting Medium

A catalyst-supporting medium is used in the F-T reactor. A common medium is a hydrocarbon mixture C_5-C_7 . Instead of purchasing fresh medium, it is desired to use a portion of a hydrocarbon fraction (e.g., C_5-C_7) produced in the process. A particularly

attractive separation system is supercritical extraction which can be used to recover C₅-C₇ (simulated here with the model compound hexane). Supercritical fluid solvents are efficient in diffusion similar with gas and at the same time good at heat transfer and solubility like liquid. So here the process and optimization for the solvent recovery unit is analyzed. It utilizes a separating model to separate the solvent from unreacted syngas and the products produced in the F-T reaction. The simulation is compared between a flash distillation column and a Radfrac Distillation column to analyze the cost. The product composition was provided by Dr. Elbashir (N. Elbashir, Texas A&M University, Qatar, 2008, personal communication), at different reaction temperatures over an alumina supported cobalt catalyst. The conditions in the F-T reactor are syngas:solvent molar ratio = 1:1, total pressure of 45 bar while temperature was varied from 210 – 250 °C.

By controlling the flash temperature and pressures, solvent recoverability and C₁₀₊ fractions were studied as a function of the combination of temperature and pressure. Results were obtained from ASPEN simulation as shown in Figs. 5.10 and 5.11. In the previous sections it has been indicated different conditions (temperatures and pressures) will affect the products distribution, while the change in these conditions also has significant influence on the thermal characteristic of the supercritical solvents. So it's necessary to study on these conditions. From the figures it can be concluded that with temperature increase, the solvent recoverability is increased, and by decreasing pressure the solvent recoverability is increased. For the C₁₀₊ hydrocarbon components from the flash, which are sold in majority in the market as middle distillates fractions, these components compositions increase as pressures go down, and there is no too much influence by temperature. Therefore, it could be concluded that with the pressure going down, solvent recoverability can be guaranteed and C₁₀₊ components fractions increase, and the flowsheet for this process is shown in Fig. 5.12.

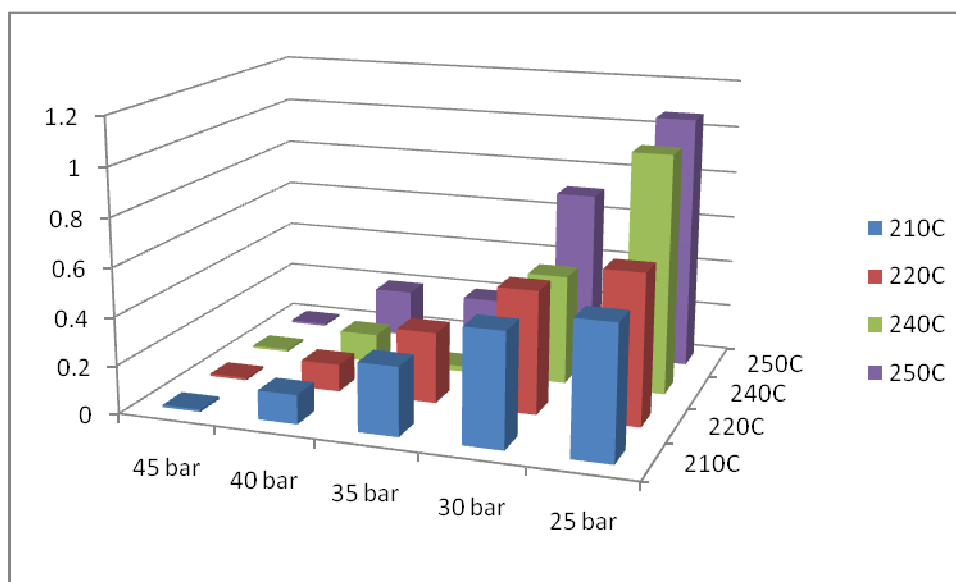


Figure 5.10. Solvent recoverability from the flash as a function of temperature and pressure

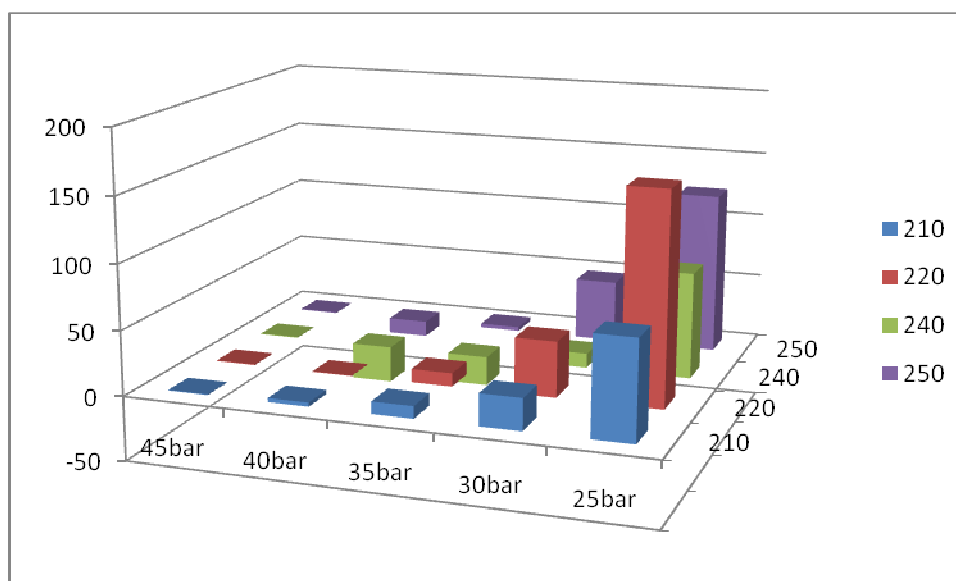


Figure 5.11. C₁₀₊ increase with temperature and pressure change in the flash

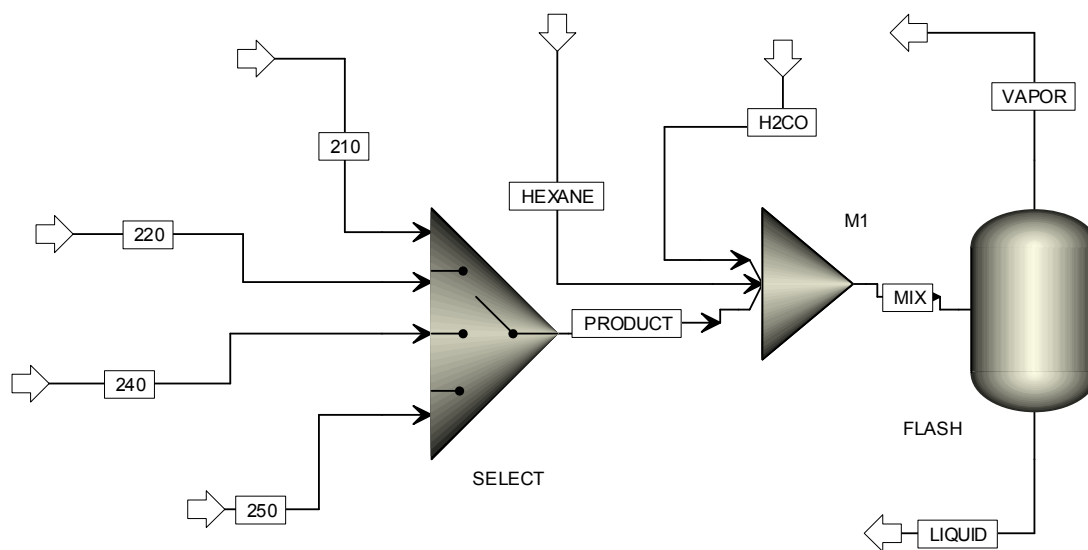


Figure 5.12. Flowsheet for solvent recovering

There are different types of separation units that could be applied to separate hexane from liquid product. Leading among those are distillation and flash separation. Both options were modeled and their costs were evaluated using the software ICARUS as shown in Table 5.11. As can be seen, flash separation is superior to distillation.

Table 5.11. Comparison between a distillation column and a flash unit

Type	Fixed Cost (\$)	Hexane purity
Radfrac Distillation column	39.5 million	94.6%
Flash2	4.3 million	93.4%

5.5.3 Management of Water

Basically, from the simulation 2.9 million kg/hr water is generated in the process, in which 600,000 kg/hr water should be separated with the syncrude with the volume ratio to be 0.7. Then, reverse osmosis is used to clean it up. The cost of water treatment is taken as 0.2 \$/m³. The recovered water can be either used inside the process for steam, or outside the process for irrigation purposes or for use in other industrial facilities. Taking the selling price of treated water to be 0.4\$/tonne, the process can save 22.6 million \$/yr from water management.

5.5.4 CO₂ Separation

In the step of F-T reaction, there is some CO₂ produced from the water gas shift reaction. Such CO₂ should be separated from the product gas and fed back to the autothermal reactor to contact the methane and produce syngas, both to increase the productivity and to reduce the greenhouse emissions. The cost is obtained from literature (Singhal and Singhal, 2000) for one pilot plant reducing CO₂ in 2000. Since the reported data were for a different size and year, the following equations are applied to normalize the result. The recycling of CO₂ is listed in Table 5.12 and the cost for separating CO₂ is indicated in Table 5.13.

$$\frac{\text{operating}_A}{\text{operating}_B} = \frac{\text{capacity}_A}{\text{capacity}_B} \quad (5.7)$$

$$\frac{FCI_A}{FCI_B} = \left(\frac{\text{capacity}_A}{\text{capacity}_B}\right)^{0.6} \quad (5.8)$$

Table 5.12. CO₂ separation and recycling

Compare	Production (kg/hr)
Before recycling	476,430
After CO ₂ recycling	570,000
Increase	19.6%

Table 5.13. Estimation of CO₂ separation cost

	Total capital investment (\$)	Total annual operating cost (\$/yr)	Capacity (Mt/yr)
Cost from literature (Singhal, 2000)	467,200,000	30,980,000	4.6
Cost for the case study	79,428,000	1,616,000	0.24

5.6 Total Cost for GTL Plant

There are wide variations in the estimates of the capital investment of a GTL plant². Some estimates are reported to be \$20,000 – 30,000 per daily barrel produced (<http://www.chemlink.com.au/gtl.htm>). Based on reported data of a Shell GTL plant in Qatar called the Pearl Plant with a 140,000 bbl/day capacity, there are different reported capital costs ranging from \$5 billion (<http://www.siteselection.com/ssinsider/snapshot/sf040202.htm>) to \$12-18 billion (http://uk.reuters.com/article/UK_SMALLCAPSRPT/idUKL3064135320071030). The total capital investment of a 140,000 bbl/day plant is \$12 to 18 billion. These numbers translate to \$36,000 (in the case of \$5 billion) to \$86,000 (in the case of \$12 billion) to \$129,000 (in the case of \$18 billion) per daily barrel produced. Assuming that the fixed capital investment is 85% of the total capital investment and by choosing the \$12 billion figure, the fixed cost of the 140,000 bbl/day plant is \$10.2 billion. In this case study, the product rate is 128,000 bbl/day. The fixed cost is calculated to be 9.67 billion dollars, and the total capital investment is thus 11.3 billion dollars.

The fixed and operating capital cost is evaluated by Aspen Icarus. The fixed cost is not so accurate since the plant size is beyond the normal capacity Aspen can simulate. Therefore the fixed cost is calculated from literature reported. The result for the GTL

² Qatar plant price is available at <http://www.chemlink.com.au/gtl.htm>, <http://www.siteselection.com/ssinsider/snapshot/sf040202.htm>, http://uk.reuters.com/article/UK_SMALLCAPSRPT/idUKL3064135320071030.

plant is shown in the following. Before calculating, the price for the product and utilities are listed in Table 5.14 for August 2008 to compare. EIA is Energy Information Administration, ICIS provides information with chemical prices.

Table 5.14. Price for August 2008 (EIA, ICIS, 2008³)

Diesel	3.29\$/gal
Naphtha	2.5\$/gal
Heating oil	3.5\$/gal
Natural gas	8.3\$/MMBtu
Electricity	0.064\$/ kWh

Working capital investment is set as 15% of total capital investment. Before calculating the operating cost, the raw material cost and utility cost are first listed as in Table 5.15 and Table 5.16. Then the comparison of annual operating cost for integration effect is illustrated in Table 5.17. GTL products sales are listed in Table 5.18. The total annualized cost is in Table 5.19 indicates that the plant makes money. LPG indicates liquefied petroleum gas, FCI indicates fixed capital investment, TCI indicates total capital investment, MMBtu stands for million British thermal unit.

Table 5.15. Costs of raw materials

Raw Materials	Cost	Flowrate (kg/hr)	Annual Cost (\$/yr)
Natural Gas	0.4 \$/kg	900,000	3,153,600,000
Water	0.4 \$/ton	1,195,020	4,187,000
Oxygen	0.138 \$/kg	990,000	1,196,791,000
Air	-	-	23,000
Total			4,354,601,000

³ EIA (Energy Information Administration) information is available at <http://www.eia.doe.gov> accessed on August 2008. ICIS pricing is available at <http://www.icis.com> accessed in August 2008.

Table 5.16. Costs of heating and cooling utilities

Heat exchanger	Utility	Utility flowrate	Utility cost	Annual utility cost (\$/yr)
Cool1	Cooling Water	11,091,787 lb/hr	0.4 \$/ton	479,165,000
Cool2	Cooling Water	724,741 lb/hr	0.4 \$/ton	31,308,000
Heat1	Heating oil	721 gal/hr	3.5 \$/gal	605,640,000
Heat2	High pressure steam	30,190 lb/hr	6.8 \$/MMBtu	65,431,000
Total				1,181,545,000

Table 5.17. Calculation of annual operating cost and savings with process integration

Items	Cost (\$/yr)
Raw Materials Cost	4,354,601,000
Operating Labor Cost	600,000
Maintenance Cost	135,000
Supervision	280,000
Electricity	1,380,000
Heating and Cooling Utilities	1,181,545,000
Catalyst	5,185,000
Total before integration	5,543,727,000
Savings from process integration	
heat integration	884,449,000
water recovering	22,629,000
Power cogeneration	93,627,000
LP saved	153,000,000
Total savings from process integration	1,153,705,000
Total operating cost with process integration	4,390,022,000

A reduction in the cost of natural gas or an increase in the unit selling price of the liquid products will render the process profitable. It is worth noting that if the company owns

its own gas wells or if special discounts in the cost of natural gas are given to the company by the host country, the GTL process can indeed be profitable.

Table 5.18. Sales of GTL products

Products	Production	Price	Annual sales (\$/yr)
Diesel	150,930 gal/hr	3.29 \$/gal	3,972,477,000
LPG	6,840 gal/hr	1.62 \$/gal	88,646,000
Naphtha	67,470 gal/hr	2.51 \$/gal	1,354,797,000
Total			5,415,921,000

Table 5.19. TAC calculation for GTL plant

Items	value
capacity	128,365 BPD
useful life period	20 years
FCI (\$)	9.67 billion
TCI (\$)	11.3 billion
total operating cost before integration(\$/yr)	5,543,727,000
total operating cost after integration(\$/yr)	4,390,022,000
total production income (\$/yr)	5,415,921,000
salvage value (\$)	0.967 billion
Depreciation/annualized fixed cost (\$/yr)	0.43 billion
total annualized cost (TAC) (\$/yr)	4.82 billion

a. ROI calculating

$$\text{The } ROI = \frac{\text{profit}}{TCI} \times 100\% = (5.4 - 4.82) / 11.3 = 5.1\% \quad (5.9)$$

This return of investment (ROI) is so low that it seems not so profitable. However, in gas-producing countries like Qatar this is attractive because the actual cost of natural gas will be much less than the market selling price. For instance, if the cost of natural gas is set at 5 \$/thousand SCF, the cost of raw materials is reduced to 3.1 billion \$/yr. This

means that the TAC is reduced to 3.576 billion \$/yr, while other fixed and operating costs remain the same. In this case, the ROI is calculated to be:

$$ROI = \frac{\text{profit}}{TCI} \times 100\% = (5.4 - 3.576) / 11.3 = 16.2\% \quad (5.10)$$

b. Break even point calculating

The process profitability is strongly dependent on the plant capacity. To illustrate this point, let us start with a relatively small GTL plant producing 4,300 BPD. The raw material cost is in Table 5.20 and operating cost is in Table 5.21. The results shown in Table 5.22 indicate that such a process will lead to a financial loss. In order to find out what the production rate leading to profit, a break-even point analysis is carried out as shown by Fig. 5.13.

Table 5.20. Raw material cost for 4,300 BPD capacity

Raw Materials	Cost	Flowrate (kg/hr)	Annual Cost (\$/yr)
Natural Gas	0.4 \$/kg	30000	105,120,000
Water	0.4 \$/ton	39834	127,000
Oxygen	0.138 \$/kg	33000	36,432,000
Air	-	-	23,000
Total			141,702,000

Table 5.21. Operating cost for the 4,300 BPD capacity

Items	Cost (\$/yr)
Raw Materials Cost	141,702,000
Operating Labor Cost	320,000
Maintenance Cost	116,000
Supervision	280,000
Electricity	42,000
Heating and Cooling Utilities	39,384,000
Catalyst	172,000
Total before integration	182,018,000
Savings from process integration	
heat integration	29,481,000
water recovering	754,000
Power cogeneration	619,000
LP saved	184,000
Total savings from process integration	31,040,000
Total operating cost with process integration	150,977,000

Table 5.22. TAC calculation for the different sizes

Items	value	value
capacity	128,000 BPD	4,300 BPD
useful life period	20 years	20 years
FCI (\$)	9.67 billion	1.26 billion
TCI (\$)	11.4 billion	1.48 billion
total operating cost before integration(\$/yr)	5,543,727,000	182,000,000
total operating cost after integration(\$/yr)	4,390,022,000	150,977,000
total production income (\$/yr)	5,415,921,000	180,500,000
salvage value (\$)	0.935 billion	0.13 billion
Depreciation/annualized fixed cost (\$/yr)	0.43 billion	0.0567 billion
total annualized cost (TAC) (\$/yr)	4.82 billion	0.2 billion

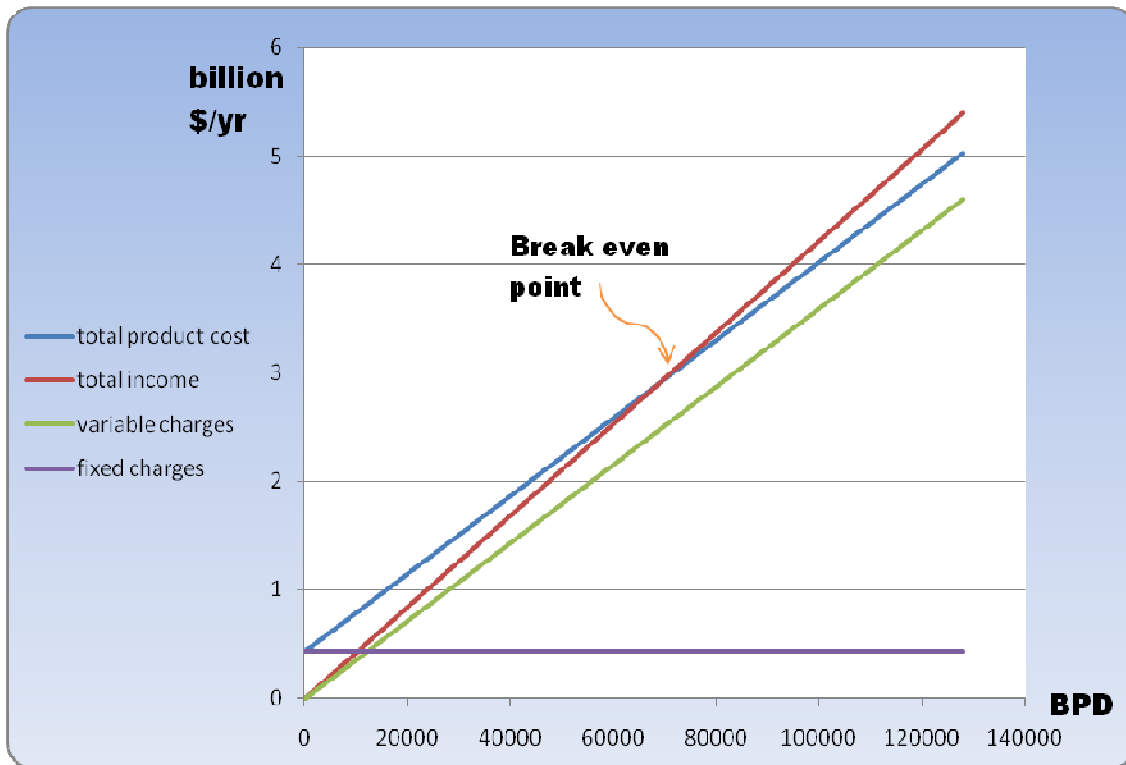


Figure 5.13. Break-even point calculation

From Fig. 5.13, it can be noticed that at production rates of 68,000 BPD, the total product cost line crosses with the total income line, which means at that point the cost breaks even, while at production rates bigger than this point, the total income line goes over the total product cost line, indicating the plant begins to make profit. The higher the capacity the more profitable the plant can be.

6 CONCLUSIONS AND RECOMMENDATIONS

This work has provided a framework for analyzing and improving the performance of F-T GTL plants. The following tasks have been performed:

- A typical GTL process has been synthesized.
- The design and operating conditions for the process has been optimized by controlling the feed ratio, the various heating and cooling utilities, and the masses.
- A thermal pinch analysis has been applied to get the optimum heating and cooling utilities.
- Integration of heat engine with HEN has been examined and cogeneration has been undertaken to generate power simultaneously with the production of different pressure header steam requirement.
- Mass integration has been conducted to recycle the tail gases, to recover the catalyst-supporting medium, and to manage process water.
- ASPEN Plus and ICARUS have been used in evaluating the performance and cost of the process.

A case study has been developed to assess a GTL plant using 1.16 billion SCF/day of natural gas to produce 128,000 barrel/day of products.

- Simulation, optimization, and integration activities have been applied. Some of the key results include:
 - Heat integration leads to a reduction in cost of 884,449,000 \$/yr
 - Cogeneration gives reduction in cost of 246,000,000 \$/yr
 - Water management provides cost savings of 22,629,000 \$/yr

- Depending on the price of natural gas, the return on investment ranges from 5.1% to 16.2% for the cost of natural gas being \$8 and 5/1000 SCF, respectively. With reduction in the cost of natural gas (because of market conditions, production conditions, or special contractual terms) or the increase in the selling prices of the liquid fuels, the process can make higher profit. A break-even point analysis indicated that under current market conditions, the production capacity should be at least 68,000 BPD to make profit. Larger plant sizes provide more profit.

The following recommendations are suggested for future work:

- Strategies to reduce greenhouse gas (GHG) emissions from the GTL plant
- Scale up strategies and analysis should be carried out
- Combination of an air separation unit (ASU) with the process will give more detailed energy configuration since the ASU consumes a large part of energy in this process
- Flexibility analysis to check the changes in the process design and operation with changing production rates and quality of the feedstocks
- Integration of GTL plants with LNG plants

REFERENCES

- Adegoke, A. A., 2006. Utilizing the Heat Content of Gas to Liquids by Products Streams for Commercial Power Generation. M.S. thesis, Petroleum Engineering, Texas A&M University, College Station, TX.
- Al-Sobhi, S., 2007. Simulation and Integration of LNG Processes. M.S. thesis, Chemical Engineering, Texas A&M University, College Station, TX.
- Ahon, V.R., Costa, E.F., Monteagudo, J.E.P., Fontes, C.E., Biscaia, E.C., et al., 2005. A Comprehensive Mathematical Model for the Fischer-Tropsch Synthesis in Well-Mixed Slurry Reactors. *Chemical Engineering Science*. 60, 677-694.
- Brumby, A., Verhelst, M., Cheret, D., 2005. Recycling GTL Catalysts -- A New Challenge. *Catalysis Today*. 106, 166-169.
- Cao, Y., Gao, Z., Jin, J., Zhou, H., Cohron, M., et al., 2008. Synthesis Gas Production with an Adjustable H₂/CO Ratio through the Coal Gasification Process: Effects of Coal Ranks and Methane Addition. *Energy and Fuels*. 22, 1720-1730.
- Chedid, R., Kobrosly, M., Ghajar, R., 2007. The Potential of Gas-to-Liquid Technology in the Energy Market: The Case of Qatar. *Energy Policy*. 35, 4799-4811.
- Cooke, J., 2003. Plant Design and Engineering. Fundamentals of Gas to Liquids, 2003, ed. Soutar E. and Deaville J., Petroleum Economist, London, United Kingdom, 20-21. Available at http://www.fwc.com/publications/tech_papers/files/peGTLp20-21.pdf.
- Cornelissen, R. L., Hirs, G.G., 1998. Exergy Analysis of Cryogenic Air Separation. *Energy Conversion and Management*. 39, 1821-1826.
- Crook, J., 2007. Pearl-The World's Largest GTL Plant. *Chemical Engineer*. May, 29-31.
- Davis, B. H., 2002. Overview of Reactors for Liquid Phase Fischer-Tropsch Synthesis. *Catalysis Today*. 71, 249-300.
- Davis, B. H., 2005. Fischer-Tropsch Synthesis: Overview of Reactor Development and Future Potentialities. *Topics in Catalysis*. 32, 143-168.
- Dry, M.E., 1981. The Fischer-Tropsch Synthesis. *Catalysis Science and Technology*, vol. 1, 1981, ed. Anderson, J.R. and Boudart, M., Springer-Verlag, New York, 159-255.

Dry, M. E., 1982. Sasol's Route to Fuels. *Chemical Engineering Technology*. 12, 744-750.

Dry, M. E., 2003. *Encyclopedia of Catalysis*. John Wiley and Sons, New York.

Elbashir, N.O., Roberts, C.B., 2005. Enhanced Incorporation of α -Olefins in the Fischer-Tropsch Synthesis Chain-Growth Process over an Alumina-Supported Cobalt Catalyst in Near-Critical and Supercritical Hexane Media. *Industrial Engineering Chemistry Research*. 44, 505-521.

El-Halwagi, M. M., 2006. *Process Integration*. Process Systems Engineering Series, Vol 7, Academic Press, San Diego, CA.

Five Winds International Inc., 2004. Gas to Liquids Life Cycle Assessment Synthesis. Report, web information available at http://www.shell.com/static/shellgasandpower-en/downloads/products_and_services/what_is_gtl/benefits_of_gtl/gtl_lca_synthesis_report.pdf.

Fox, J.M., 1990. Fischer-Tropsch Reactor Selection. *Catalysis Letters*. 7, 281-292.

Freerks, R., 2003. Early Efforts to Upgrade Fischer-Tropsch Reaction Products into Fuels, Lubricants, and Useful Materials. AIChE Spring National Meeting, New Orleans, LA.

Government of Qatar, 2007. Turning Qatar into a Competitive Knowledge Based Economy. Qatar Knowledge Economy Project, online available at <http://siteresources.worldbank.org/KFDLP/Resources/QatarKnowledgeEconomyAssessment.pdf>

GTL Task Force Department, 2001. Gas to Liquids Industry Development. Department of Industry, Science and Researches, Canberra ACT, 2001. A discussion paper available http://www.ret.gov.au/resources/fuels/alternative_transport_fuels/Documents/GTL_DiscussionPaper.pdf

Hall, K.R., 2005. A New Gas to Liquids or Gas to Ethylene Technology. *Catalysis Today*. 106, 243-246.

Halstead, K., 2006. Oryx GTL: A Case Study. *Chemical Engineer*. July, 34-36.

Hao, X., Djatmiko, M.E., Xu, Y., Wang, Y., Chang, J., 2008. Simulation Analysis of a Gas-to-Liquid Process Using Aspen Plus. *Chemical Engineering Technology*. 31, 188-196.

Hodge, C., 2003. Comment: More Evidence Mounts for Banning, not Expanding, Use of Ethanol in US Gasoline. *Oil and Gas Journal*. 101, 18-20.

Hoek, A., 2005. The Shell GTL Process: Towards a World Scale Project in Qatar. *Chemie Ingenieur Technik*. 8, 77.

Iandoli, C.L., Kjelstrup, S., 2007. Exergy Analysis of a GTL Process Based on Low-Temperature Slurry F-T Reactor Technology with a Cobalt Catalyst. *Energy and Fuels*. 21, 2317-2324.

Ijeomah, C.E., Dandekar, A.Y., Chukwu, G.A., Khataniar, S., Patil, S.L., et al., 2008. Measurement of Wax Appearance Temperature under Simulated Pipeline Conditions. *Energy and Fuels*. 22, 2437-2442.

Iliuta, I., Ortiz-Arroyo, A., Larachi, F.L.F., Grandjean, B.P.A., Wild, G., 1999. Hydrodynamics and Mass Transfer in Trickle-Bed Reactors: An Overview. *Chemical Engineering Science*. 54, 5329-5337.

Jaramillo, P., 2007. A Life Cycle Comparison of Coal and Natural Gas for Electricity Generation and the Production of Transportation Fuels. PhD dissertation, Civil and Environmental Engineering, Carnegie Mellon University, Pittsburgh, PA.

Jarosch, K.T., Tonkovich, A.L.Y., Perry, S.T., Kuhlmann, D., Yong, W., 2005. Microchannel Reactors for Intensifying Gas-to-Liquid Technology. *American Chemical Society*. 914, 258-272.

Jory, R., 2006. GTL Fues: Driving the Growth of the GTL Market. 23th World Gas Conference, Amsterdam.

Khoshnoodi, M., 1997. Simulation of Partial Oxidation of Natural Gas to Synthesis Gas Using ASPEN PLUS. *Fuel Processing Technology*. 50, 275-289.

Koo, K.Y., Roh, H., Yu, T.S., Seo, D.J., Yoon, W.L., et al., 2008a. Coke Study on MgO-Promoted Ni/Al₂O₃ Catalyst in Combined H₂O and CO₂ Reforming of Methane for Gas to Liquid (GTL) Process. *Applied Catalysis A: General*. 340, 183-190.

Koo, K.Y., Roh, H., Yu, T.S., Seo, D.J., Yoon, W.L., et al., 2008b. A Highly Effective and Stable Nano-Sized Ni/MgO-Al₂O₃ Catalyst for GTL Process. *International Journal of Hydrogen Energy*. 33, 2036-2043.

Krishna, R., Ellenberger, J., Sie, S.T., 1996. Reactor Development for Conversion of Natural Gas to Liquid Fuels: A Scale up Strategy Relying on Hydrodynamic Analogies. *Chemical Engineering Science*. 51, 2041-2050.

Krishna, R., Sie, S.T., 2000. Design and Scale-up of the Fischer-Tropsch Bubble Column Slurry Reactor. *Fuel Processing Technology*. 64, 73-105.

Krishna, R., van Baten, J. M., Urseanu, M.I., 2000a. Three Phase Eulerian Simulations of Bubble Column Reactors Operating in the Churn Turbulent Regime: A Scale up Strategy. *Chemical Engineering Science*. 55, 3275-3286.

Krishna, R., Urseanu, M. I., Dreher, A.J., 2000b. Gas Hold up in Bubble Columns: Influence of Alcohol Addition versus Operation at Elevated Pressures. *Chemical Engineering Science*. 39, 371-378.

Krishna, R., van Baten, J.M., Urseanu, M.I., Ellenberger, J., 2001a. A Scale up Strategy for Bubble Column Slurry Reactors. *Catalysis Today*. 66, 199-207.

Krishna, R., van Baten, J.M., Urseanu, M.I., Ellenberger, J., 2001b. Design and Scale up of a Bubble Column Slurry Reactor for Fischer-Tropsch Synthesis. *Chemical Engineering Science*. 56, 537-545.

Krishna, R., van Baten, J.M., 2003. Mass Transfer in Bubble Columns. *Catalysis Today*. 79-80, 67-75.

Kuipers, E.W., Scheper, C., Wilson, J.H., Winkenburg, I.H., Oosterbeek, H., 1996. Non-ASF Product Distributions due to Secondary Reactions during Fischer-Tropsch Synthesis. *Journal of Catalysis*. 158, 288-300.

Kurevija, T., Kukulj, N., Rajkovic, D., 2007. Global Prospects of Synthetic Diesel Fuel Produced from Hydrocarbon Resources in Oil and Gas Exporting Countries. *Rudarsko-Geolosko-naftni Zbornik*. 19, 79-86.

Larsson, M., 2007. An Experimental Study of Fischer-Tropsch Fuels in a Diesel Engine. B.S. thesis, Applied Mechanics, Chalmers University of Technology, Gothenburg, Sweden.

Levenspiel, O., 2002. Modeling in Chemical Engineering. *Chemical Engineering Science*. 57, 4691-4696.

Liu, H., You, L., 1999. Characteristics and Applications of the Cold Heat Exergy of Liquefied Natural Gas. *Energy Conversion and Management*. 40, 1515-1525.

Liu, W., Huang, Z., Wang, J., Qiao, X., Hou, J., 2008. Effects of Dimethoxy Methane Blended with Gas to Liquid on Particulate Matter Emissions from a Compression Ignition Engine. *Energy and Fuels*. 22, 2307-2313.

Lu, Y., Lee, T., 2007. Influence of the Feed Gas Composition on the Fischer-Tropsch Synthesis in Commercial Operations. *Journal of Natural Gas Chemistry*. 16, 329-341.

Maiti, S.N., Eberhardt, J., Kundu, S., Cadenhouse-beaty, P.J., Adams, D.J., 2001. How to Efficiently Plan a Grassroots Refinery. *Hydrocarbon Process.* 80, 43-49.

Maretto, C., 2001. Design and Optimization of a Multi-Stage Bubble Column Slurry Reactor for Fischer-Tropsch Synthesis. *Catalysis Today.* 66, 241-248.

Maretto, C., Piccolo, S., Krishna, R., 2001. Hydrodynamics, Design and Scale-up of a Multi-Stage Bubble Column Slurry Reactor for Fischer-Tropsch Synthesis. 6th World Congress of Chemical Engineers, Melbourne, Australia.

Nouri, S., Kaggerud, K., 2006. Waste-to-Plastics: Process Alternatives. Report, Energy and Environment, Norwegian University of Science and Technology, Trondheim, Norway.

Patel, B., 2005. Gas Monetisation: A Techno-Economic Comparison of Gas to Liquid and LNG." 7th World Congress of Chemical Engineering, Glasgow, Scotland, UK.

Perry, R.H., Green, 1984. *Perry's Chemical Engineers' Handbook.* McGraw-Hill Inc., San Francisco, CA.

Rahmin, I.I., 2003. Gas-to-Liquid Technologies: Recent Advances, Economics, Prospects. 26th Annual International Conference, Prague, Czech Republic. Available at <http://www.gtlpetrol.com/public/iirahmim2003prague.pdf>.

Reddy, K.T., Basu, S., 2007. Gas-to-Liquid Technologies: India's Perspective. *Fuel Processing Technology.* 88, 493-500.

Rentech Inc., 2005. The Economic Viability of an FT Facility Using PRB Coals. Presentation to the Wyoming Governor's Office available at http://www.wyomingbusiness.org/pdf/energy/WBC_Public_Presentation_4-14-05.pdf

Repasky, J. M., Reader, R.T., 2004. In Enhanced Heat Transfer Reformer Technology for GTL Applications, Proceedings of AIChE Spring Meeting Conference, New Orleans, LA. American Institute of Chemical Engineers, New York, NY, 1504-1508.

Saxena, S.C., 1995. Bubble Column Reactors and Fischer-Tropsch Synthesis. *Catalyst Reviews: Science and Engineering.* 37, 227.

Sehabiague, L., Lemoine, R., Behkish, A., Heintz, Y.J., Sanoja, M., et al., 2008. Modeling and Optimization of a Large-Scale Slurry Bubble Column Reactor for Producing 10,000 bbl/day of Fischer-Tropsch Liquid Hydrocarbons. *Journal of Chinese Institute of Chemical Engineers.* 39, 169-179.

Sie, S.T., Krishna, R., 1999. Fundamentals and Selection of Advanced Fischer-Tropsch Reactors. *Applied Catalysis A: General*. 186, 55-70.

Singhal, R.K., Singhal, A.K.M., 2000. Environmental Issues and Management of Waste in Energy and Mineral Production. Taylor and Francis, Alberta, Canada.

Smith, A.R., Klosed, J., 2001. A Review of Air Separation Technologies and Their Integration with Energy Conversion Processes. *Fuel Processing Technology*. 70, 115-134.

Song, X., Sayari, A., 1996. Sulfated Zirconia as a Cocatalyst in Fischer-Tropsch Synthesis. *Energy and Fuels*. 10(3), 561-565.

Soterious, A., Ignacio, E., 1983. A Structural Optimization Approach in Process Synthesis. *Computers and Chemical Engineering*. 7, 723-734.

Spath, P.L., Dayton, D.C., 2003. Preliminary Screening-Technical and Economic Assessment of Synthesis Gas to Fuels and Chemicals with Emphasis on the Potential for Biomass-Derived Syngas. Report, National Renewable Energy Laboratory (NREL), Golden, CO.

Steynberg, A.P., Espinoza, R.L., Jager, B. Vosloo, A.C., 1999. High Temperature Fischer-Tropsch Synthesis in Commercial Practice. *Applied Catalysis A: General*. 186, 41-54.

Steynberg, A.P., Dry, M.E., 2004. Fischer-Tropsch Technology. Elsevier. Amsterdam, the Netherlands.

Suehiro, Y., Nakamura, A., Sacomota, A., 2004. New GTL Process- Best Candidate for Reduction of CO₂ in Natural Gas Utilization. SPE Asia Pacific Oil and Gas Conference and Exhibition, Perth, Australia, 1423-1429.

Tam, S.S. Stanton, M.E., Ghose, S., Deppe, G., Spencer, D.F. A High Pressure Carbon Dioxide Separation Process for IGCC Plants. Source is available at www.netl.doe.gov/publications/proceedings/01/carbon_seq/1b4.pdf.

Tijmensen, M. J.A., Faaij, A.P.C., Hamelinck, C.N., van Hardeveld, M.R.M., 2002. Exploration of the Possibilities for Production of Fischer Tropsch Liquids and Power via Biomass Gasification. *Biomass and Bioenergy*. 23(2), 129-152.

Urseanu, M.I., Guit, R.P.M., Stankiewicz, A., van Kranenburg, G., Lommen, J.H.G.M., 2003. Influence of Operating Pressure on the Gas Hold up in Bubble Columns for High Viscous Media. *Chemical Engineering Science*. 58, 697-704.

Van der Laan, G., 1999. Kinetics, Selectivity and Scale up of the Fischer-Tropsch Synthesis. PhD dissertation, Chemical Engineering, University of Groningen, Groningen, Netherlands.

Vandu, C.O., Krishna, R., 2004. Influence of Scale on the Volumetric Mass Transfer Coefficients in Bubble Columns. *Chemical Engineering Science*. 43, 575-579.

Vessia, O. 2005. Biofuels from lignocellulosic Material. Project report, Electrical Engineering, Norwegian University of Science and Technology, Trondheim, Norway.

Vosloo, A.C., 2001. Fischer-Tropsch: A Futuristic View. *Fuel Processing Technology*. 71, 149-155.

Wang, X., 2004. Computer Simulation of GTL and Various Problems in Thermodynamics. PhD dissertation, Chemical Engineering, Texas A&M University, College Station, TX.

Wang, Y., Xu, Y., Li, Y., Zhao, Y., Zhang, B., 2003. Heterogeneous Modeling for Fixed Bed Fischer-Tropsch Synthesis: Reactor Model and Its Applications. *Chemical Engineering Science*. 58, 867-875.

Weeden, S., 2001. Special Report-GTL: Progress and Prospects: Financial Commitments Brighten. *Oil and Gas Journal*. 99(11), 58.

Wesenberg, M.H., 2006. Gas Heated Steam Reformer Modeling. PhD dissertation, Chemical Engineering, Norwegian University of Science and Technology, Trondheim, Norway.

Wilhelm, D. J., Simbeck, D.R., Karp A.D., Dickenson R.L., 2001. Syngas Production for Gas-to-Liquids Applications: Technologies, Issues and Outlook. *Fuel Processing Technology*. 71, 139-148.

Wu, T., Huang, Z., Zhang, W., Fang, J., Qi, Y., 2007. Physical and Chemical Properties of GTL-Diesel Fuel Blends and Their Effects on Performance and Emissions of a Multicylinder DI Compression Ignition Engine. *Energy and Fuels*. 21, 1908-1914.

Yagi, F., Kanai, R., Wakamatsu, S., Kajiyama, R., Suehiro, Y., et al., 2005. Development of Synthesis Gas Production Catalyst and Process. *Catalysis Today*. 104, 2-6.

Zhang, J., Zhu, X., 2000. Simultaneous Optimization Approach for Heat Exchanger Network Retrofit with Process Changes. *Industrial Engineering Chemistry Research*. 39, 4963-4973.

Zhang, N., 2000. Novel Modeling and Decomposition for Overall Refinery Optimization and Debottlenecking. PhD dissertation, Chemical Engineering, University of Manchester Institute of Science and Technology, Manchester, England.

VITA

Name: Buping Bao

Address: Artie McFerrin Department of Chemical Engineering
Texas A&M University
College Station, TX 77843-3136

Email address: bupingbb@gmail.com

Education: B.S., Chemical Engineering, 2006
Zhejiang University, Hangzhou, P.R.China
M.S., Chemical Engineering, 2008
Texas A&M University